Virus Research 147 (2010) 77–84

Contents lists available at ScienceDirect

Virus Research

journal homepage: www.elsevier.com/locate/virusres

Overall linkage map of the nonstructural proteins of Aichi virus

Kumiko Ishikawa[a,b], Jun Sasaki[a,*], Kazuyuki Hiratsuka[b], Koki Taniguchi[a]

[a] Department of Virology and Parasitology, Fujita Health University School of Medicine, Dengakugakubo 1-98, Kutsukake-cho, Toyoake, Aichi 470-1192, Japan
[b] Graduate School of Environment and Information Science, Yokohama National University, Tokiwadai 79-7, Hodogaya-ku, Yokohama, Kanagawa 240-8501, Japan

ARTICLE INFO

Article history:
Received 2 July 2009
Received in revised form 8 October 2009
Accepted 17 October 2009
Available online 30 October 2009

Keywords:
Aichi virus
Picornavirus
Genus *Kobuvirus*
Protein linkage map
Mammalian two-hybrid

ABSTRACT

Aichi virus (AiV), which is associated with acute gastroenteritis in humans, is a member of the genus *Kobuvirus* of the family *Picornaviridae*. Picornavirus genome replication occurs in replication complexes that include viral nonstructural proteins, host proteins and viral RNA. In poliovirus, all nonstructural proteins are found in the replication complexes, suggesting the ability of the viral nonstructural proteins to interact with each other. In this study, we examined the interactions between the AiV nonstructural proteins using a mammalian two-hybrid system. The results showed that all of the tested proteins could interact with more than one protein. We observed homodimerization of five proteins, bidirectional heterodimerization of six protein pairs, and unidirectional heterodimerization of eighteen protein pairs. Among the interactions detected in this study, the 2A–2B, 2A–2BC, 2A–2C, 2BC–3CD, 2BC–3C, 2C–3C, 2C–3CD and 3AB–3C interactions have not been observed in the previous two-hybrid studies with other picornaviruses. The strongest interaction was observed between 2A and 3CD. AiV 2A has already been shown to be involved in genome replication. Domain mapping of the 2A and 3CD interaction in mammalian two-hybrid analysis revealed that the C-terminal quarter of 2A is not required for the interaction with 3CD.

1. Introduction

Picornaviruses are small, nonenveloped, positive-sense, single-stranded RNA viruses. The family *Picornaviridae* is currently classified into eight genera and includes many important human and animal pathogens such as poliovirus (PV), hepatitis A virus, rhinovirus, and foot-and-mouth disease virus. The genome of picornaviruses is 7200–8500 nucleotides in length, and contains a 5′-terminal covalently linked protein, VPg, and a 3′-terminal poly(A) tail. The genome has a single large open reading frame (ORF), which consists of a capsid-coding region, P1, and nonstructural protein-coding regions, P2 and P3. The P1 region encodes VP4, VP2, VP3 and VP1, while the P2 and P3 regions encode 2A, 2B, 2C, 3A, 3B, 3C and 3D. Some viruses encode a leader (L) protein upstream of the P1 region. After virus proteins have been translated as a single large polyprotein from the ORF, the polyprotein is processed by virus-encoded proteases into various functional proteins. The cleavage intermediates, 2BC, 3AB and 3CD, have functions distinct from those of the mature cleavage products. Of the nonstructural proteins, 3B, 3C and 3D are functionally conserved among different genera of picornaviruses, i.e. VPg, protease and RNA-dependent RNA polymerase, respectively (Racaniello, 2006). For 2C, motifs characteristic of nucleoside triphosphate-binding proteins are highly conserved among picornaviruses (Gorbalenya et al., 1990; Racaniello, 2006). 2B, 2C, 2BC, 3A and 3AB have been identified as membrane-associated proteins in several genera (Knox et al., 2005; Krogerus et al., 2007; Teterina et al., 1997; Towner et al., 1996). In contrast, L and 2A vary in amino acid sequence and function among genera.

Aichi virus (AiV) is a member of the genus *Kobuvirus* of the family *Picornaviridae*. AiV was first isolated in 1989 from a stool specimen from a patient with oyster-associated gastroenteritis in Aichi, Japan (Yamashita et al., 1991). The virus has been detected not only in Japan, but also in other Asian countries, Europe, Brazil and Africa (Ambert-Balay et al., 2008; Goyer et al., 2008; Oh et al., 2006; Pham et al., 2007; Yamashita et al., 1995). The proteins encoded by AiV have some unique features. The capsid protein VP0 is present in mature viral particles devoid of cleavage into VP2 and VP4 (Yamashita et al., 1998). The L protein of AiV exhibits no homology to those of other picornaviruses (Yamashita et al., 1998), and has been indicated to be involved in viral RNA replication and encapsidation (Sasaki et al., 2003). AiV 2A, as well as 2A of human parechoviruses, is related to a cellular protein, H-rev107 (Hughes and Stanway, 2000). Recently, it was indicated that AiV 2A is not a protease and that it is involved in viral RNA replication (Sasaki and Taniguchi, 2008).

Picornavirus infection induces rearrangement of intracellular membrane structures, and replication of the genome occurs in replication complexes associated with the rearranged membrane structure (Bienz et al., 1987, 1990, 1992). Replication complexes

* Corresponding author. Tel.: +81 562 93 2486; fax: +81 562 93 4008.
E-mail address: jsasaki@fujita-hu.ac.jp (J. Sasaki).

0168-1702/$ – see front matter © 2009 Elsevier B.V. All rights reserved.
doi:10.1016/j.virusres.2009.10.009

Table 1
Nucleotide sequences of the primers used in this study. The MluI sites and parts of the EcoRV sites are underlined; stop codons are indicated in bold type.

Name	Sense	Sequence	Position
L-Fw	+	5′-CGACGCGTGGATGGCTGCAACACGGGTTTCAC-3′	744–765
L-Rv	–	5′-ATCTCATTGCCGTTGGAGGTTAGTGG-3′	1234–1253
2A-Fw	+	5′-CGACGCGTGGGGCGCCGCCTCAGCGACTC-3′	3792–3810
2A-Rv	–	5′-ATCTCACTGTCGCCTGATGCCTGGG-3′	4181–4199
2B-Fw	+	5′-CGACGCGTGGGGTCTCCTCACCCTCTCTGC-3′	4200–4219
2B-Rv	–	5′-ATCTCAATCTCATTGAGGTTCAAGGGTTGCCC-3′	4675–4694
2C-Fw	+	5′-CGACGCGTGGGGGCTCAAAGACTTCAACG-3′	4695–4713
2C-Rv	–	5′-ATCTCACTGGCGTCTGATGAGGGAGG-3′	5680–5699
3A-Fw	+	5′-CGACGCGTGGGGCAACCGGGTCATCGACGC-3′	5700–5719
3A-Rv	–	5′-ATCTCATTGAGGTTCCTGTGGCGTG-3′	5966–5984
3B-Rv	–	5′-ATCTCATGGCGCTGGATGTGACGAG-3′	6046–6065
3C-Fw	+	5′-CGACGCGTGGGGAATCTCCCCTGCTGTCCC-3′	6066–6085
3C-Rv	–	5′-ATCTCATTGTTGGGTAGTGGCAAATTG-3′	6615–6635
3D-Fw	+	5′-CGACGCGTCTCTCATTGTTCCCACTGC-3′	6636–6655
3D-Rv	–	5′-ATCTCAGGCAGCCAGCAGATTTAG-3′	8022–8042
2AΔ1-Fw	+	5′-CGACGCGTGGGCCCCCGACGGCAGTGC-3′	3891–3907
2AΔ2-Fw	+	5′-CCCTCCCATTGGACCCTTGC-3′	3993–4012
2AΔ2-Rv	–	5′-CACCTTGCCGGATGGCCCAG-3′	3872–3890
2AΔ3-Fw	+	5′-TCCCTCCCCAACACCGGC-3′	4092–4109
2AΔ3-Rv	–	5′-GAGAATTTCGAGGTAAGG-3′	3975–3992
4170P	+	5′-GTGAAAGCGCTCCCAGGCATCAGG-3′	4170–4193
4103M	–	5′-GTTGGGGAGGGATTCGCCAGTG-3′	4082–4103

contain viral proteins, host proteins and viral RNA (Bienz et al., 1987, 1990, 1992; Belov et al., 2005; Rust et al., 2001; Schlegel et al., 1996). In PV, all nonstructural proteins are found in replication complexes, suggesting that the viral nonstructural proteins interact with each other (Egger et al., 1996). Studies to reach a more holistic understanding of interactions between viral nonstructural proteins have been carried out in PV (Cuconati et al., 1998; Teterina et al., 2006b; Xiang et al., 1998; Yin et al., 2007), coxsackievirus B3 (CV-B3) (de Jong et al., 2002), and porcine teschovirus (PTV) (Zell et al., 2005) by using a yeast two-hybrid system or a mammalian two-hybrid system. These studies have demonstrated different protein–protein interactions between genera.

In this study, we analyzed protein–protein interactions between AiV nonstructural proteins utilizing a mammalian two-hybrid system. The results showed that all of the AiV nonstructural proteins tested have the ability to interact with at least one protein. We observed homodimerization of five proteins, bidirectional heterodimerization of six protein pairs, and unidirectional heterodimerization of eighteen protein pairs. These interactions included ones that have not been observed in previous two-hybrid studies with other picornaviruses, such as the 2A–2B, 2A–2BC, 2A–2C, 2BC–3CD, 2BC–3C, 2C–3C, 2C–3CD and 3AB–3C interactions. The strongest interaction was observed between 2A and 3CD. To further clarify the molecular properties of 2A, we examined the domain of 2A required for binding to 3CD by mammalian two-hybrid analysis using a series of 2A deletion mutants. The results showed that the C-terminal 23 amino acids were not essential for the interaction with 3CD.

2. Materials and methods

2.1. Cells

Vero cells were maintained in Eagle's minimum essential medium supplemented with 5% fetal bovine serum at 37 °C.

2.2. Plasmids

Mammalian two-hybrid analysis was performed using a Checkmate system (Promega). Plasmids pBIND and pACT from the system contain the yeast GAL4 DNA-binding domain and the herpes simplex virus type 1 VP16 activation domain, respectively. The pBIND plasmid also contains the gene of *Renilla* luciferase, which is used to monitor transfection efficiency. A reporter plasmid, pG5luc, expresses firefly luciferase under the control of a minimal TATA box and five GAL4 binding sites. The coding regions of the nonstructural proteins and cleavage intermediates, L, 2A, 2B, 2BC, 2C, 3A, 3AB, 3C and 3D, were amplified by PCR from a full-length cDNA clone, pAV-FL (Sasaki et al., 2001). The 3C and 3CD sequences carrying a C143A mutation that abolishes the 3C protease activity were amplified by PCR from pMAL-3CDmut (Nagashima et al., 2008). The sequences of the primers used are shown in Table 1. The amplified fragments, which contained an MluI site at the 5′ end and a stop codon followed by a part of the EcoRV site at the 3′ end, were digested with MluI, and cloned into the MluI–EcoRV sites of pACT, and then the nucleotide sequences of the inserts of the derived plasmids were confirmed. The derived plasmids were called pACT-L, -2A, -2B, -2BC, -2C, -3A, -3AB, -3C, -3Cm (which contains the C143A mutation), -3CD and -3D. Each MluI–EcoRV fragment derived from these pACT constructs was inserted into the same sites of pBIND, yielding pBIND-L, -2A, -2B, -2BC, -2C, -3A, -3AB, -3C, -3Cm, -3CD and -3D.

2.3. 2A deletion mutants

The sequence from nucleotide (nt) 3891 to the C-terminus of the 2A-coding region was amplified by PCR with primers 2AΔ1-Fw and 2A-Rv (Table 1) using pAV-FL as the template. The derived fragment was cloned into pACT and pBIND as described above, yielding pACT-2AΔ1 and pBIND-2AΔ1. Deletions of nt 3891–3992 (2AΔ2) and nt 3993–4091 (2AΔ3) were introduced by inverse PCR with the primers shown in Table 1 using pACT-2A as a template. The PCR products were self-ligated, and the MluI–EcoRV fragments of the derived plasmids were cloned into these sites of pACT and pBIND, yielding pACT-2AΔ2 and -2AΔ3 and pBIND-2AΔ2 and -2AΔ3. A deletion of nt 4104–4169 (2AΔ4) was introduced by inverse PCR with the primers shown in Table 1 using a plasmid containing nt 3642–5328 as a template. The resultant fragment was self-ligated, and then PCR was performed using the derived plasmid as a template with primers 2A-Fw and 2A-Rv. The PCR product was digested with MluI, and cloned into pACT and pBIND. The resultant plasmids were named pACT-2AΔ4 and pBIND-2AΔ4. The nucleotide sequences of the 2A regions of all of the 2A deletion mutants were verified.

2.4. Mammalian two-hybrid analysis

Vero cells were seeded at 2.4×10^5 cells per well in 24-well plates 18 h before transfection. The cells were cotransfected with 0.4 μg each of pBIND or one of its derivatives, pACT or one of its derivatives and pG5luc using lipofectamine and PLUS transfection reagents (Invitrogen). At 48 h post transfection, cells were lysed in passive lysis buffer (Promega), and then firefly and *Renilla* luciferase activities were determined using a Dual-luciferase reporter assay system (Promega) with a luminometer, Lumat LB9507 (Berthold). Relative luciferase activity was defined as the ratio of firefly luciferase activity to *Renilla* luciferase activity. All assays were performed at least three times.

2.5. Western blotting

Vero cells were grown in 6-well plates and then transfected with 1.6 μg of pACT constructs or pBIND constructs per well using lipofectamine and PLUS reagents. At 48 h after transfection, cell lysates were prepared, and proteins were separated by SDS-polyacrylamide gel electrophoresis (PAGE), transferred to polyvinylidene difluoride membranes, and then reacted with a monoclonal anti-VP16 antibody (Santa Cruz) or a monoclonal antibody against the N-terminal domain of GAL4 (Zymed). After the membranes had been incubated with a horseradish peroxidase-conjugated secondary antibody, chemiluminescence signals were visualized using ECL Advance reagent (Amersham Biosciences) and LAS1000 (Fujifilm).

3. Results and discussion

3.1. Expression of the GAL4- and VP16-fusion viral nonstructural proteins in Vero cells

To investigate the interactions between the viral nonstructural proteins by a mammalian two-hybrid assay, we constructed plasmids that express the nonstructural proteins and the cleavage intermediates as fusion proteins with the DNA-binding domain of the yeast GAL4 protein (pBIND-L, -2A, -2B, -2BC, -2C, -3A, -3AB, -3C, -3CD and -3D) or with the transcription activation domain of the herpes simplex virus type 1 VP16 protein (pACT-L, -2A, -2B, -2BC, -2C, -3A, -3AB, -3C, -3CD and -3D). Since the preliminary two-hybrid assay using pBIND-3C or pACT-3C resulted in a marked reduction in *Renilla* luciferase activity (data not shown), we used protease-inactivated mutants, pBIND-3Cm and pACT-3Cm, in the following experiments.

Prior to a two-hybrid assay, the constructed plasmids were individually transfected into Vero cells and then the expression of each fusion protein was determined by Western blotting using the anti-GAL4 antibody or anti-VP16 antibody. All fusion proteins were detected in the expected molecular masses, albeit the expression levels were different (Fig. 1).

3.2. A mammalian two-hybrid assay

To analyze the interactions between the viral nonstructural proteins, Vero cells were transfected with all possible combinations of the pBIND constructs and pACT constructs together with the pG5luc reporter plasmid, and then luciferase activities were measured. As controls, luciferase activities obtained with the combination of the viral protein gene-bearing pBIND plasmid and the empty pACT plasmid and that of the empty pBIND plasmid and the viral protein gene-bearing pACT plasmid were used. According to previously reported criteria (Teterina et al., 2006b), we defined luciferase activity that was 4-fold or more than the higher of the two control values as a positive interaction and considered 2- to 3-fold increases in the ones as possibly indicative of interactions (Fig. 2B).

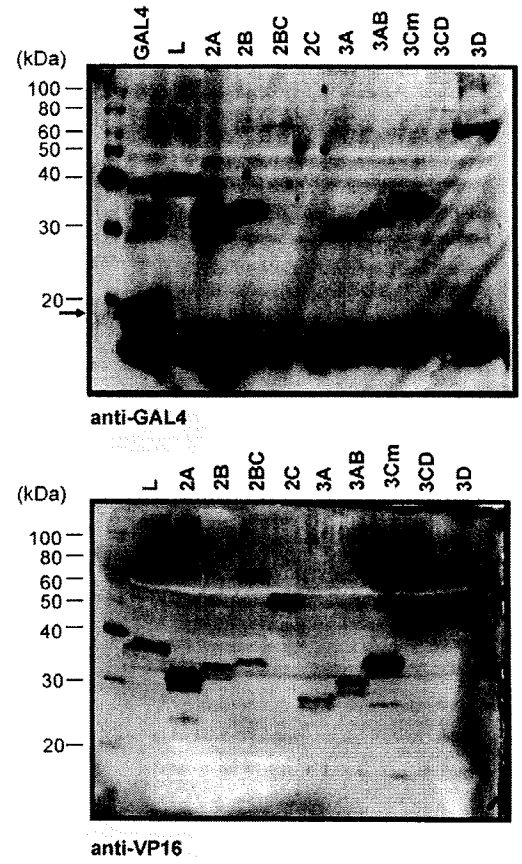

Fig. 1. Expression of the GAL4- and VP16-fusion proteins in Vero cells. pBIND (top panel) and pACT (bottom panel) encoding the indicated nonstructural proteins were individually transfected into Vero cells. At 48 h after transfection, cell lysates were prepared, and proteins were separated by SDS-PAGE and blotted onto polyvinylidene difluoride (PVDF) membranes. The blots were reacted with a monoclonal antibody specific for the GAL4 DNA-binding domain or the VP16 activation domain. The positions of molecular markers are indicated on the left of each panel. An arrowhead indicates the position of the intact GAL4 protein.

The results of the assay are shown in Fig. 2A and Table 2. Moreover, the detected interactions were compared with those detected on two-hybrid analyses of other picornaviruses (Table 3). We observed the homodimerization of five proteins (2A, 2B, 2BC, 2C and 3A), the bidirectional heterodimerization of six protein

Table 2
Linkage map of the AiV nonstructural proteins. The degree of the increase in luciferase activity over the control: ±, 2- to 3-fold; +, 4- to 8-fold; ++, >10-fold; +++, >100-fold.

DNA-binding domain fusion (pBIND)	Activation domain fusion (pACT)									
	L	2A	2B	2BC	2C	3A	3AB	3Cm	3CD	3D
L	–	–	–	–	–	–	–	–	–	–
2A	–	±	±	+	+	±	–	+	++	±
2B	–	–	++	+	–	–	–	–	–	–
2BC	–	–	+	+	++	++	++	–	–	–
2C	–	–	+	++	++	+	±	–	–	–
3A	–	–	+	+	±	±	–	–	–	–
3AB	–	–	–	–	–	±	–	–	–	–
3Cm	+	±	–	++	++	–	+	–	–	–
3CD	±	+++	–	++	++	–	+	–	–	–
3D	–	–	–	–	–	–	–	–	–	–

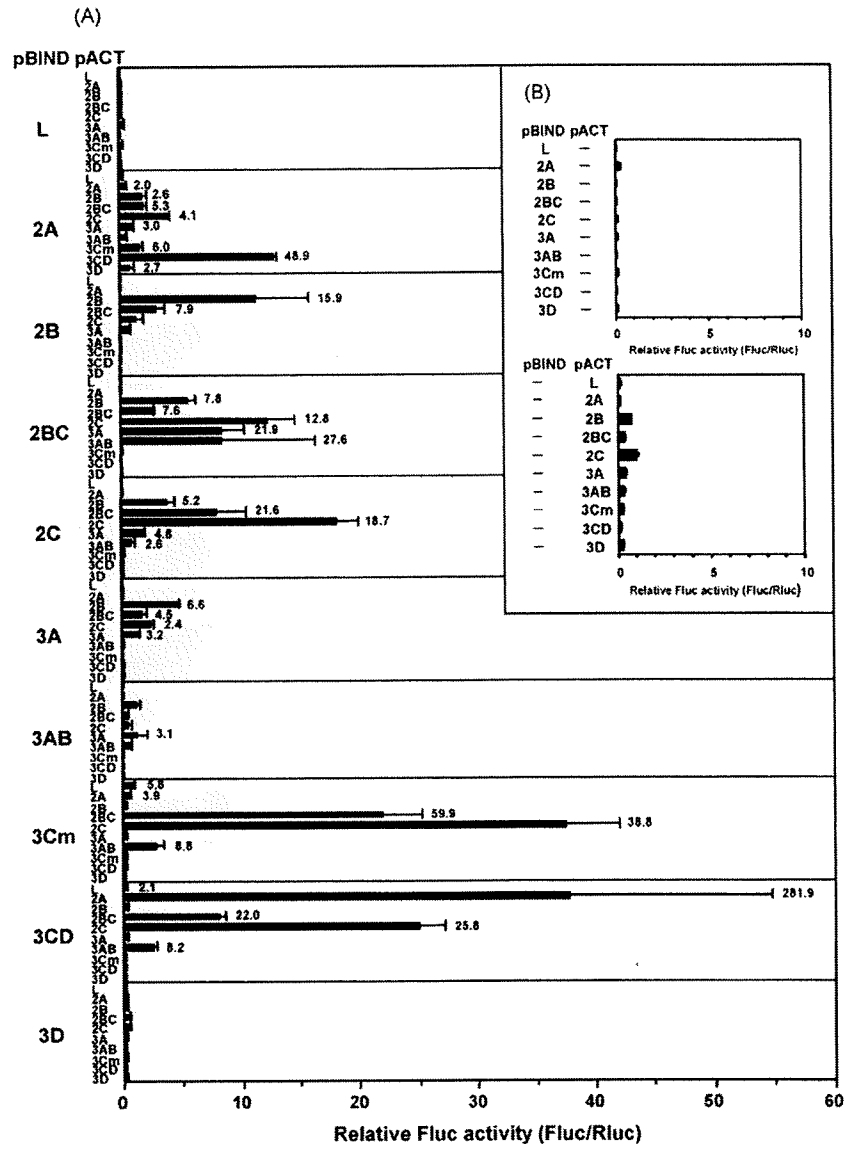

Fig. 2. Luciferase activity induced in the presence of GAL4- and VP16-fusion proteins (A) and control experiments (B). The indicated combinations of pBIND containing the GAL4 DNA-binding domain and pACT containing the VP16 activation domain were transfected into Vero cells together with pG5luc. Cell lysates were prepared at 48 h after transfection and assayed for firefly luciferase activity. Transfection efficiency was normalized by the activity of *Renilla* luciferase (Rluc), which was simultaneously expressed from pBIND. The data are represented as means ± SD of the relative luciferase activities (Fluc/Rluc) in at least three independent experiments. Luciferase activities obtained on transfection of the combination of the viral protein gene-bearing pBIND plasmid and the empty pACT plasmid (indicated by a hyphen), and that of the empty pBIND plasmid (indicated by a hyphen) and the viral protein gene-bearing pACT plasmid were used as controls. For positive interactions, the fold-increase in the relative luciferase activity compared to the higher of the two control values is indicated on the right side of the bar.

pairs (2A–3CD, 2A–3C, 2BC–2B, 2BC–2C, 2BC–3A and 2C–3A), and the unidirectional heterodimerization of eighteen protein pairs. 2A interacted with the largest number of proteins, eight. Conversely, 3D showed a weak interaction only with 2A, and L interacted only with 3C and 3CD. The interactions of eight protein pairs, 2A–2B, 2A–2BC, 2A–2C, 2BC–3C, 2BC–3CD, 2C–3C, 2C–3CD and 3AB–3C, have not been observed in the previous two-hybrid studies with other picornaviruses.

All combinations of P2–P2 protein interactions and thirteen pairs of P2–P3 protein interactions were detected. Also in PV, various combinations of P2–P3 interactions have been observed in mammalian and yeast two-hybrid assays, while in PTV, no P2–P3 interactions have been detected on yeast two-hybrid analysis (Table 3).

On the other hand, P3–P3 interactions were observed with only four protein pairs in this study. In particular, no homo- or heterodimerization between 3C, 3CD and 3D was detected. The inability of 3C, 3CD and 3D to interact with each other observed in this study did not seem to be due to the expression levels of these proteins, because on Western blotting, efficient expression was detected for the GAL4- and VP16-3C proteins, and the GAL4- and VP16-3D proteins (Fig. 2A). For the GAL4-3CD and VP16-3CD proteins, the expression levels were relatively low, but the interactions with P2 proteins led to high levels of luciferase activity. This result was in contrast to that with PTV, in which all interactions between 3C, 3CD and 3D have been observed. In PV, the 3CD–3CD, 3D–3CD and 3D–3D interactions have been detected on yeast two-hybrid analysis, and the 3C–3C and 3C–3D interactions have been

observed on in vitro analyses (Pathak et al., 2007; Xiang et al., 1998). In addition, it has been suggested that the homodimerization of 3C or 3CD and the 3C–3D interaction are required for cre-dependent VPg uridylylation (Pathak et al., 2002, 2007; Shen et al., 2007). Further studies may be required to assess the interactions between 3C, 3CD and 3D of AiV.

3.3. The interactions between 2A and 3CD

AiV 2A has no homology to the 2A proteases of enteroviruses and no NPGP sequence, which is required for the cleavage at the 2A/2B junction in aphtho-, cardio-, erbo- and teschoviruses (Yamashita et al., 1998). AiV 2A, like parechovirus and avian encephalomyelitis virus 2A, has been reported to be related to the H-rev107 family of proteins (Hughes and Stanway, 2000). Recently, AiV 2A was shown to be involved in viral RNA replication (Sasaki and Taniguchi, 2008).

The data presented here demonstrated that 2A interacted with all of the tested nonstructural proteins except for L and 3AB, although the homodimerization of 2A and heterodimerization with 2B, 3A or 3D resulted in only 2- to 3-fold increases in the luciferase level. Notably, the interaction of 2A with 3CD was the strongest among the interactions detected in this study. The exact roles of AiV 3CD in virus replication have not been established yet, but PV 3CD has been shown to bind to viral RNA and to be involved in RNA replication, besides its role as a protease (Franco et al., 2005; Gamarnik and Andino, 2000; Harris et al., 1994; Herold and Andino, 2001). Thus, the 2A–3CD interaction in AiV may play a role in RNA replication.

To characterize this interaction in detail, we attempted to determine the interaction domain of 2A required for binding to 3CD. We generated a series of 2A deletion mutants, 2AΔ1, 2AΔ2, 2AΔ3 and 2AΔ4, as shown in Fig. 3A. Western blotting showed that the expression levels of 2AΔ2, 2AΔ3 and 2AΔ4 were similar to that of the wild type, while that of 2AΔ1 was slightly less than that of the wild type (Fig. 3B). Then we performed mammalian two-hybrid analysis with the combinations of pBIND-2AΔ1, -2AΔ2, -2AΔ3 or -2AΔ4 and pACT-3CD or those of pACT-2AΔ1, -2AΔ2, -2AΔ3 or -2AΔ4 and pBIND-3CD. As a result, no interaction of 2AΔ1, 2AΔ2 and 2AΔ3 with 3CD was observed, whereas 2AΔ4 still exhibited reciprocal interactions with 3CD at levels comparable to those in the case of the wild-type 2A (Fig. 3C). We concluded from this result that the C-terminal quarter (amino acids [aa] 105–127) of the 2A

Table 3
Comparison of protein–protein interactions between nonstructural proteins observed in different picornaviruses. CV-B3, coxsackievirus B3; PV-1, poliovirus 1; PTV-1, porcine teschovirus 1. +, interaction; –, no interaction; ND, not done.

Type	Protein pair	Mammalian two-hybrid			Yeast two-hybrid	
		AiV	CV-B3 (de Jong et al., 2002)	PV-1 (Teterina et al., 2006b)	PV-1 (Cuconati et al., 1998; Xiang et al., 1998; Yin et al., 2007)	PTV-1 (Zell et al., 2005)
L–P3	L-3C	+				+
	L-3CD	+				+
P2–P2	2A–2A	+	ND	ND	+	ND
	2A–2B	+	ND	ND	–	ND
	2A–2BC	+	ND	ND	–	ND
	2A–2C	+	ND	ND	–	ND
	2B–2B	+	+	+	+	+
	2B–2BC	+	+	+	+	+
	2B–2C	+	+	+	+	+
	2C–2C	+	–	+	–	–
	2BC–2BC	+	+	+	+	–
	2BC–2C	+	+	+	+	–
P2–P3	2A–3A	+	ND	ND	+	ND
	2A–3C	+	ND	ND	+	ND
	2A–3CD	+	ND	ND	+	ND
	2A–3D	+	ND	ND	+	ND
	2B–3A	+	ND	+	+	–
	2B–3AB	–	ND	+	+	–
	2BC–3A	+	ND	+	–	–
	2BC–3AB	+	ND	+	–	–
	2BC–3C	+	ND	ND	–	–
	2BC–3CD	+	ND	ND	–	–
	2C–3A	+	ND	+	+	–
	2C–3AB	+	ND	–	+	–
	2C–3C	+	ND	ND	–	–
	2C–3CD	+	ND	ND	–	–
P3–P3	3A–3A	+	ND	+	+	+
	3A–3AB	+	ND	+	+	–
	3A–3C	–	ND	ND	–	–
	3A–3CD	–	ND	ND	–	–
	3A–3D	–	ND	ND	–	–
	3B–3CD	ND	ND	ND	+	ND
	3B–3D	ND	ND	ND	+	ND
	3AB–3AB	–	ND	–	+	–
	3AB–3C	+	ND	ND	–	–
	3AB–3CD	+	ND	ND	+	–
	3AB–3D	–	ND	ND	+	–
	3C–3C	–	ND	ND	–	+
	3C–3CD	–	ND	ND	–	+
	3C–3D	–	ND	ND	–	+
	3CD–3CD	–	ND	ND	+	+
	3D–3CD	–	ND	ND	+	+
	3D–3D	–	ND	ND	+	+

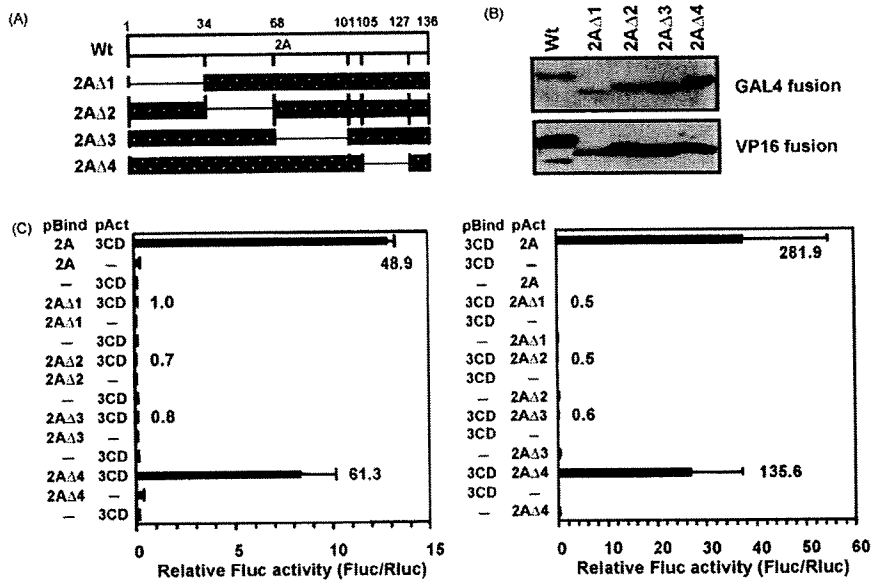

Fig. 3. Deletion analysis of the AiV 2A protein. (A) Schematic representation of the wild type and various 2A deletion mutants. The deleted regions are shown by lines. Wt, wild type. (B) Expression of various 2A mutants fused to the GAL4 DNA-binding domain or the VP16 activation domain in Vero cells. Wt 2A and 2AΔ1, 2AΔ2, 2AΔ3 and 2AΔ4 cloned in pBIND and pACT were transfected into Vero cells, and then the expression of the GAL4- (top) and VP16- (bottom) fusion proteins was analyzed by Western blotting as described in the legend to Fig. 1. (C) Mammalian two-hybrid analysis of interactions between the 2A deletion mutants and 3CD. Vero cells were cotransfected with the indicated pBIND and pACT plasmids, together with the pG5luc plasmid. The luciferase assay was performed as described in the legend to Fig. 2.

sequence was not required for the interaction with 3CD. This region, deleted in 2AΔ4, has been previously reported to correspond to a conserved motif in the H-rev107 family of proteins, which is referred to as the hydrophobic region (aa 105–127) (Hughes and Stanway, 2000).

It has not been determined yet whether the 2A protein of human parechovirus 1 (HPeV-1), which is 150 aa long, is essential for virus replication. However, it has been reported that it binds to the 3′-untranslated region of the viral RNA, and the N-terminal aa 43–56 region and the C-terminal region downstream of the hydrophobic region have been mapped as the important regions for RNA binding (Samuilova et al., 2004). Additionally, HPeV-1 2A is localized in both the nucleus and the cytoplasm in infected cells, and is partially colocalized with viral RNA in the perinuclear region (Samuilova et al., 2004). These findings suggest that HPeV-1 2A is present at the sites of viral RNA replication. 2A related to H-rev107 may play important roles in replication complexes through interactions with 3CD or various viral proteins and viral RNA during viral RNA replication.

3.4. The interactions between 2B, 2BC, 2C, 3A and 3AB

2B, 2BC, 2C, 3A and 3AB are known as membrane-associated proteins in different picornavirus genera (Knox et al., 2005; Krogerus et al., 2007; Teterina et al., 1997; Towner et al., 1996). In the case of PV, 2BC and 3A are thought to be involved in the alteration of cellular membrane structures in infected cells (Cho et al., 1994; Suhy et al., 2000). Interactions between these proteins have been detected in mammalian and yeast two-hybrid analyses and in vitro experiments (Cuconati et al., 1998; de Jong et al., 2002; Teterina et al., 2006b; Xiang et al., 1998; Yin et al., 2007). In addition, genetic analyses have suggested the importance of the 3AB (or 3A)–2B, 2B–2C and 2C–3A interactions. It has also been reported that differences in the binding of 2C to 2B or 3A affect membrane morphology induced by PV infection (Teterina et al., 2006a,b).

In AiV, interactions between these proteins were observed with all combinations except for 2B–3AB and 3AB–3AB, and of these interactions, the 2C–2C, 2BC–2C, 2BC–3A and 2BC–3AB interactions caused a significant stimulation of the luciferase signals (>18-fold more than the control). Although we have not examined whether these proteins of AiV exhibit affinity for membranes, analysis utilizing the TMpred program (Hofmann and Stoffel, 1993) predicted the existence of transmembrane domains in 2B and 3A (data not shown). Also in AiV, the interactions between these proteins might be important for membrane rearrangement and formation of replication complexes.

3.5. Interactions of 2C and 2BC with 3C and 3CD

The 2C–3C, 2C–3CD, 2BC–3C and 2BC–3CD interactions caused high luciferase activity by 22- to 60-fold, albeit in one orientation. The 2B–3C, 2B–3D and 2C–3D interactions were not detected, suggesting that interaction between the 2C region and the 3C region was responsible for the observed 2C–3CD, 2BC–3C and 2BC–3CD interactions. Although these interactions have not been detected on yeast two-hybrid analyses in PV and PTV, PV 2C has been shown to inhibit the 3C protease activity, and the interaction of 2C with 3C has been observed in vitro (Banerjee et al., 2004). The 2C–3C and 2BC–3C interactions observed in our study may have a similar effect on the 3C activity. In addition, considering that PV 3CD is involved in RNA replication, it would be interesting to determine whether the interaction of 2C or 2BC with 3CD plays a role in RNA replication.

All of the 2C–3C, 2C–3CD, 2BC–3C and 2BC–3D interactions were unidirectional: no activation of luciferase expression was detected with the combination of GAL4-2BC and VP16-3Cm or -3CD or the combination of GAL4-2C and VP16-3Cm or -3CD. This is not likely to be due to relatively poor expression of the GAL4-2BC and GAL4-2C proteins, because the homodimerization of 2BC or 2C and the combinations of GAL4-2BC or -2C and VP16-2B or -3A produced increased luciferase activity. In these fusion proteins, the fused GAL4 or VP16 sequences may interfere with proper folding of the viral proteins and thereby may affect protein interactions.

3.6. L–3C and L–3CD interactions

The AiV L protein exhibits no significant homology in amino acid sequence to other picornaviral L proteins (Yamashita et al.,

1998). Although we have already shown that the AiV L protein is involved in viral RNA replication and encapsidation (Sasaki et al., 2003), the detailed functions of this protein in these steps have not been determined yet. In this study, L interacted only with 3C and 3CD in one orientation, and the interaction with 3CD was very weak (2.1-fold above the control). Also for the L protein of PTV, which exhibits no homology to AiV L, interactions with 3C and 3CD have been reported (Zell et al., 2005). At present, it is difficult to predict how these interactions are required for viral RNA replication and encapsidation.

4. Conclusion

In this study, we observed a network of protein–protein interactions involving all of the AiV nonstructural proteins, which includes unique combinations that have not been observed in the two-hybrid studies with other picornavirus genera. The mammalian two-hybrid assay has been used extensively to study protein–protein interactions. On the other hand, additional approaches such as pull-down or coimmunoprecipitation assays will be required to further validate this assay.

The detected interactions may provide not only a better understanding of the AiV life cycle but also a means to elucidate the potential, but as yet unidentified, functions of the nonstructural proteins, some of which are functionally conserved among different picornaviruses. It will be of interest to investigate the relationship between the protein–protein interactions detected and virus replication.

Acknowledgments

This work was supported in part by Grants-in-Aid from the Ministry of Education, Culture, Sports, Science and Technology and from the Ministry of Health, Labor and Welfare.

References

Ambert-Balay, K., Lorrot, M., Bon, F., Giraudon, H., Kaplon, J., Wolfer, M., Lebon, P., Gendrel, D., Pothier, P., 2008. Prevalence and genetic diversity of Aichi virus in community and hospitalized patients. J. Clin. Microbiol. 46, 1252–1258.

Banerjee, R., Weidman, M.K., Echeverri, A., Kundu, P., Dasgupta, A., 2004. Regulation of poliovirus 3C protease by the 2C polypeptide. J. Virol. 78, 9243–9256.

Belov, G.A., Fogg, M.H., Ehrenfeld, E., 2005. Poliovirus proteins induce membrane association of GTPase ADP-ribosylation factor. J. Virol. 79, 7207–7216.

Bienz, K., Egger, D., Pasamontes, L., 1987. Association of polioviral proteins of the P2 genomic region with the viral replication complex and virus-induced membrane synthesis as visualized by electron microscopic immunocytochemistry and autoradiography. Virology 160, 220–226.

Bienz, K., Egger, D., Troxler, M., Pasamontes, L., 1990. Structural organization of poliovirus RNA replication is mediated by viral proteins of the P2 genomic region. J. Virol. 64, 1156–1163.

Bienz, K., Egger, D., Pfister, T., Troxler, M., 1992. Structural and functional characterization of the poliovirus replication complex. J. Virol. 66, 2740–2747.

Cho, M.W., Teterina, N., Egger, D., Bienz, K., Ehrenfeld, E., 1994. Membrane rearrangement and vesicle induction by recombinant poliovirus 2C and 2BC in human cells. Virology 202, 129–145.

Cuconati, A., Xiang, W., Lahser, F., Pfister, T., Wimmer, E., 1998. A protein linkage map of the P2 nonstructural proteins of poliovirus. J. Virol. 72, 1297–1307.

de Jong, A.S., Schrama, I.W.J., Willems, P.H.G.M., Galama, J.M.D., Melchers, W.J.G., van Kuppeveld, F.J.M., 2002. Multimerization reactions of coxsackievirus proteins 2B, 2C and 2BC: a mammalian two-hybrid analysis. J. Gen. Virol. 83, 783–793.

Egger, D., Pasamontes, L., Bolten, R., Boyko, V., Bienz, K., 1996. Reversible dissociation of the poliovirus replication complex: functions and interactions of its components in viral RNA synthesis. J. Virol. 70, 8675–8683.

Franco, D., Pathak, H.B., Cameron, C.E., Rombaut, B., Wimmer, E., Paul, A.V., 2005. Stimulation of poliovirus synthesis in a HeLa cell-free in vitro translation-RNA replication system by viral protein 3CDpro. J. Virol. 79, 6358–6367.

Gamarnik, A.V., Andino, R., 2000. Interactions of viral protein 3CD and poly(rC) binding protein with the 5′ untranslated region of the poliovirus genome. J. Virol. 74, 2219–2226.

Gorbalenya, A.E., Koonin, E.V., Wolf, Y.I., 1990. A new superfamily of putative NTP-binding domains encoded by genomes of small DNA and RNA viruses. FEBS Lett. 262, 145–148.

Goyer, M., Aho, L.-S., Bour, J.-B., Ambert-Balay, K., Pothier, P., 2008. Seroprevalence distribution of Aichi virus among a French population in 2006-2007. Arch. Virol. 153, 1171–1174.

Harris, K.S., Xiang, W., Alexander, L., Lane, W.S., Paul, A.V., Wimmer, E., 1994. Interaction of poliovirus polypeptide 3CDpro with the 5′ and 3′ termini of the poliovirus genome. Identification of viral and cellular cofactors needed for efficient binding. J. Biol. Chem. 269, 27004–27014.

Herold, J., Andino, R., 2001. Poliovirus RNA replication requires genome circularization through a protein–protein bridge. Mol. Cell. 7, 581–591.

Hofmann, K., Stoffel, W., 1993. TMbase—a database of membrane spanning proteins sequences. Biol. Chem. Hoppe-Seyler 347, 166.

Hughes, P.J., Stanway, G., 2000. The 2A proteins of three diverse picornaviruses are related to each other and to the H-rev107 family of proteins involved in the control of cell proliferation. J. Gen. Virol. 81, 201–207.

Knox, C., Moffat, K., Ali, S., Ryan, M., Wileman, T., 2005. Foot-and-mouth disease virus replication sites form next to the nucleus and close to the Golgi apparatus, but exclude marker proteins associated with host membrane compartments. J. Gen. Virol. 86, 687–696.

Krogerus, C., Samuilova, O., Pöyry, T., Jokitalo, E., Hyypiä, T., 2007. Intracellular localization and effects of individually expressed human parechovirus 1 nonstructural proteins. J. Gen. Virol. 88, 831–841.

Nagashima, S., Sasaki, J., Taniguchi, K., 2008. Interaction between polypeptide 3ABC and the 5′-terminal structural elements of the genome of Aichi virus: implication for negative-strand RNA synthesis. J. Virol. 82, 6161–6171.

Oh, D.-Y., Silva, P.A., Hauroeder, B., Diedrich, S., Cardoso, D.D.P., Schreier, E., 2006. Molecular characterization of the first Aichi viruses isolated in Europe and in South America. Arch. Virol. 151, 1199–1206.

Pathak, H.B., Ghosh, S.K., Roberts, A.W., Sharma, S.D., Yoder, J.D., Arnold, J.J., Gohara, D.W., Barton, D.J., Paul, A.V., Cameron, C.E., 2002. Structure–function relationships of the RNA-dependent RNA polymerase from poliovirus 3Dpol: a surface of the primary oligomerization domain functions in capsid precursor processing and VPg uridylylation. J. Biol. Chem. 277, 31551–31562.

Pathak, H.B., Arnold, J.J., Wiegand, P.N., Hargittai, M.R., Cameron, C.E., 2007. Picornavirus genome replication: assembly and organization of the VPg uridylylation ribonucleoprotein (initiation) complex. J. Biol. Chem. 282, 16202–16213.

Pham, N.T.K., Khamrin, P., Nguyen, T.A., Kanti, D.S., Phan, T.G., Okitsu, S., Ushijima, H., 2007. Isolation and molecular characterization of Aichi viruses from fecal specimens collected in Japan, Bangladesh, Thailand, and Vietnam. J. Clin. Microbiol. 45, 2287–2288.

Racaniello, V.R., 2006. Picornaviridae: the viruses and their replication. In: Knipe, D.M., Howley, P.M. (Eds.), Fields Virology, 5th ed. Lippincott, Williams & Wilkins, Philadelphia, pp. 795–838.

Rust, R.C., Landmann, L., Gosert, R., Tang, B.L., Hong, W., Hauri, H.P., Egger, D., Bienz, K., 2001. Cellular COPII proteins are involved in production of the vesicles that form the poliovirus replication complex. J. Virol. 75, 9808–9818.

Samuilova, O., Krogerus, C., Poyry, T., Hyypia, T., 2004. Specific interaction between human parechovirus nonstructural 2A protein and viral RNA. J. Biol. Chem. 279, 37822–37831.

Sasaki, J., Kusuhara, Y., Maeno, Y., Kobayashi, N., Yamashita, T., Sakae, K., Takeda, N., Taniguchi, K., 2001. Construction of an infectious cDNA clone of Aichi virus (a new member of the family *Picornaviridae*) and mutational analysis of a stem–loop structure at 5′ end of the genome. J. Virol. 75, 8021–8030.

Sasaki, J., Nagashima, S., Taniguchi, K., 2003. Aichi virus leader protein is involved in viral RNA replication and encapsidation. J. Virol. 77, 10799–10807.

Sasaki, J., Taniguchi, K., 2008. Aichi virus 2A protein is involved in viral RNA replication. J. Virol. 82, 9765–9769.

Schlegel, A., Giddings, T.H.J., Ladinsky, M.S., Kirkegaard, K., 1996. Cellular origin and ultrastructure of membranes induced during poliovirus infection. J. Virol. 70, 6576–6588.

Shen, M., Wang, Q., Yang, Y., Pathak, H.B., Arnold, J.J., Castro, C., Lemon, S.M., Cameron, C.E., 2007. Human rhinovirus type 14 gain-of-function mutants for oriI utilization define residues of 3C(D) and 3Dpol that contribute to assembly and stability of the picornavirus VPg uridylylation complex. J. Virol. 81, 12485–12495.

Suhy, D.A., Giddings Jr., T.H., Kirkegaard, K., 2000. Remodeling the endoplasmic reticulum by poliovirus infection and by individual viral proteins: an autophagy-like origin for virus-induced vesicles. J. Virol. 74, 8953–8965.

Teterina, N.L., Gorbalenya, A.E., Egger, D., Bienz, K., Ehrenfeld, E., 1997. Poliovirus 2C protein determinants of membrane binding and rearrangements in mammalian cells. J. Virol. 71, 8962–8972.

Teterina, N.L., Gorbalenya, A.E., Egger, D., Bienz, K., Rinaudo, M.S., Ehrenfeld, E., 2006a. Testing the modularity of the N-terminal amphipathic helix conserved in picornavirus 2C proteins and hepatitis C NS5A protein. Virology 344, 453–467.

Teterina, N.L., Levenson, E., Rinaudo, M.S., Egger, D., Bienz, K., Gorbalenya, A.E., Ehrenfeld, E., 2006b. Evidence for functional protein interactions required for poliovirus RNA replication. J. Virol. 80, 5327–5337.

Towner, J.S., Ho, T.V., Semler, B.L., 1996. Determinants of membrane association for poliovirus protein 3AB. J. Biol. Chem. 271, 26810–26818.

Xiang, W., Cuconati, A., Hope, D., Kirkegaard, K., Wimmer, E., 1998. Complete protein linkage map of poliovirus P3 proteins: interaction of polymerase 3Dpol with VPg and with genetic variants of 3AB. J. Virol. 72, 6732–6741.

Yamashita, T., Kobayashi, S., Sakae, K., Nakata, S., Chiba, S., Ishihara, Y., Isomura, S., 1991. Isolation of cytopathic small round viruses with BS-C-1 cells from patients with gastroenteritis. J. Infect. Dis. 164, 954–957.

Yamashita, T., Sakae, K., Kobayashi, S., Ishihara, Y., Miyake, T., Mubina, A., Isomura, S., 1995. Isolation of cytopathic small round virus (Aichi virus) from Pakistani

children and Japanese travelers from Southeast Asia. Microbiol. Immunol. 39, 433–435.
Yamashita, T., Sakae, K., Tsuzuki, H., Suzuki, Y., Ishikawa, N., Takeda, N., Miyamura, T., Yamazaki, S., 1998. Complete nucleotide sequence and genetic organization of Aichi virus, a distinct member of the *Picornaviridae* associated with acute gastroenteritis in humans. J. Virol. 72, 8408–8412.
Yin, J., Liu, Y., Wimmer, E., Paul, A.V., 2007. Complete protein linkage map between the P2 and P3 non-structural proteins of poliovirus. J. Gen. Virol 88, 2259–2267.
Zell, R., Seitz, S., Henke, A., Munder, T., Wutzler, P., 2005. Linkage map of protein–protein interactions of porcine teschovirus. J. Gen. Virol. 86, 2763–2768.

Virus Research 147 (2010) 265–274

Contents lists available at ScienceDirect

Virus Research

journal homepage: www.elsevier.com/locate/virusres

Phylogenetic and cluster analysis of human rhinovirus species A (HRV-A) isolated from children with acute respiratory infections in Yamagata, Japan

Katsumi Mizuta[a,1], Asumi Hirata[b,1], Asuka Suto[a], Yoko Aoki[a], Tadayuki Ahiko[a], Tsutomu Itagaki[c], Hiroyuki Tsukagoshi[d], Yukio Morita[d], Masatsugu Obuchi[e], Miho Akiyama[f], Nobuhiko Okabe[f], Masahiro Noda[g], Masato Tashiro[e], Hirokazu Kimura[f,*]

[a] Yamagata Prefectural Institute of Public Health, 1-6-6 Toka-machi, Yamagata-shi, Yamagata 990-0031, Japan
[b] Tochigi Prefectural Institute of Public Health and Environmental Sciences, 2154-13 Shimo-okamoto, Utsunomiya-shi, Tochigi 329-1196, Japan
[c] Yamanobe Pediatric Clinic, 2908-14 Yamanobe-machi, Higashimurayama-gun, Yamagata 990-0301, Japan
[d] Gunma Prefectural Institute of Public Health and Environmental Sciences, 371 Kamioki-machi, Maebashi-shi, Gunma 371-0052, Japan
[e] Influenza Virus Research Center, National Institute of Infectious Diseases, 4-7-1 Gakuen, Musashimurayama-shi, Tokyo 208-0011, Japan
[f] Infectious Disease Surveillance Center, National Institute of Infectious Diseases, 4-7-1 Gakuen, Musashimurayama-shi, Tokyo 208-0011, Japan
[g] Department Virology III, National Institute of Infectious Diseases, 4-7-1 Gakuen, Musashimurayama-shi, Tokyo 208-0011, Japan

ARTICLE INFO

Article history:
Received 22 July 2009
Received in revised form
13 November 2009
Accepted 19 November 2009
Available online 27 November 2009

Keywords:
Human rhinovirus species A
Phylogenetic analysis
Molecular epidemiology
Wheezy bronchiolitis
VP4/VP2 coding region

ABSTRACT

We performed phylogenetic and cluster analysis of human rhinovirus species A (HRV-A) isolated from 76 children with acute respiratory infection in Yamagata prefecture, Japan during the period 2003–2007. Phylogenetic trees based on the nucleotide and amino acid sequences of the *VP4/VP2* coding region showed that the present strains could be classified into 11 and 8 clusters, respectively. The homology among the present strains ranged from 66.6% to 100% at the nucleotide level and 84.7% to 100% at the amino acid level. The interspecies distance (mean ± standard deviation) was calculated to be 0.235 ± 0.048 at the nucleotide level and 0.076 ± 0.033 at the amino acid level. In addition, the phylogenetic trees created based on the nucleotide and amino acid sequences showed that HRV-A strains belonging to some clusters were associated with both upper respiratory infection and wheezy bronchiolitis, while other strains were associated with upper respiratory infection alone. These results suggest that the present HRV-A isolates had a wide nucleotide divergence and were associated with acute respiratory infection, including upper respiratory infection and wheezy bronchiolitis, in Yamagata prefecture, Japan during the investigation period.

1. Introduction

Human rhinoviruses (HRVs), which are positive sense-stranded RNA viruses belonging to the *Picornaviridae* family, cause acute respiratory infection (ARI) in humans and are the major pathogen for the common cold (Turner and Couch, 2007). HRV, the major pathogen for the common cold, is responsible for around 50% of asthma exacerbations and is one of the factors that can direct the infant immune system towards an asthmatic phenotype (Nicholson et al., 1993; Johnston et al., 1996; Jackson et al., 2008). In addition, accumulating evidence suggests that some patients with asthma or exacerbation of asthma may be associated with HRV infection, although the pathophysiology of this association is not clear at present (Wos et al., 2008). Thus, HRV is being reevaluated as an important agent of ARI in humans (Papadopoulos et al., 2002; Imakita et al., 2000; Wos et al., 2008).

More than 100 serotypes of HRV have been confirmed, and these viruses have been classified into many clusters on the basis of genetic analysis (Savolainen et al., 2002a,b). Recently, it was reported that HRV can be classified into 3 species (HRV-A, -B, and -C) on the basis of phylogenetic analysis of the *VP4* gene (Lau et al., 2007). Strains belonging to HRV-A and -B species are culturable and have been implicated as the most prevalent viruses associated with ARI (Savolainen et al., 2002a), whereas those of the HRV-C species are not culturable. However, the genetic characteristics and epidemiology of domestic HRV-A infection are not known. Therefore, as a general indicator of domestic infection, we performed phylogenetic and cluster analysis of HRV-A isolated from patients

* Corresponding author. Tel.: +81 42 561 0771; fax: +81 42 565 3315.
E-mail address: kimhiro@nih.go.jp (H. Kimura).
[1] Both these authors contributed equally to this work.

0168-1702/$ – see front matter © 2009 Elsevier B.V. All rights reserved.
doi:10.1016/j.virusres.2009.11.011

with ARI in Yamagata prefecture, Japan during the period 2003–2007.

2. Materials and methods

2.1. Isolates and patients

We analyzed 76 HRV-A isolates obtained from patients with upper respiratory infection (URI) (70 patients) or wheezy bronchiolitis (6 patients) referred to pediatric clinics in Yamagata prefecture during the period 2003–2007. The samples were obtained by the local health authority of Yamagata prefecture for the surveillance of viral diseases in Japan. We diagnosed URI, also known as the common cold, and URI that typically affects the upper airway which includes the nose (sinusitis), throat (pharyngitis), and voice box (laryngitis) (Cherry, 2003). Wheezy bronchiolitis was diagnosed due to the presence of wheezing alone or chest retractions in association with a URI (Robert, 2003). A detailed listing of patients and isolates is provided in Table 1. All patients were under 16 years of age (5.8 ± 3.3 years; mean ± standard deviation [SD]). No significant seasonal variation of HRV-A isolation was seen in this study.

2.2. Cell culture and virus isolation

To isolate various respiratory viruses, we used HEF, HEp-2, Vero E6, MDCK, RD-18S and GMK cells in this study. Cells were grown in Eagle's minimal essential medium (Nissui No. 3; Nissui Pharmaceutical Co., Tokyo, Japan) containing 5–10% fetal bovine serum or calf serum at 37 °C in a humidified atmosphere of 5% CO_2 (Mizuta et al., 2008). Cells were grown in 96 well microplates (Greiner Bio-One, Frickenhausen, Germany).

After the plates were washed with phosphate-buffered saline without calcium and magnesium (PBS), 100 μL of maintenance medium was added to each well of the plates. Each specimen was then centrifuged at 3000 rpm for 15 min and 75 μL of the supernatant was inoculated into 2 wells of each cell line. The inoculated plates were incubated at 33 °C in a CO_2 incubator. We observed the plates two or three times per week for cytopathic effects (CPEs) over 14 days for all cell lines, without passage or medium change (Mizuta et al., 2008). When a suspected HRV CPE was observed, we passaged and stored the cells at −80 °C until analysis. Viral identification was carried out by reverse-transcription polymerase chain reaction (RT-PCR) and sequence analysis (Savolainen et al., 2002a).

2.3. RNA extraction, RT-PCR, and sequencing

For RNA extraction, RT-PCR, and sequence analysis, infected culture fluids were centrifuged at 3000 × *g* at 4 °C for 15 min and the supernatants were used for RT-PCR and sequence analysis as described previously (Savolainen et al., 2002a; Iwai et al., 2006). Briefly, viral RNA was extracted from 140 μL supernatant with a QIAamp Viral RNA Mini Kit (Qiagen, Valencia, CA). The RT-PCR procedure was performed according to the manufacturer's instructions (Access RT-PCR System; Promega, Madison, WI). The primers for RT-PCR were as follows: 5′ GGG ACC AAC TAC TTT GGG TGT CCG TGT 3′ (9895 forward; sense [534–560 nt]), and 5′ GCA TCI GGY ARY TTC CAC CAC CAN CC 3′ (9565 reverse; antisense [1083–1058 nt]). The following protocol was used: 45 min at 48 °C (reverse transcription), 2 min at 94 °C (denaturation), and 40 cycles of 94 °C for 30 s, 60 °C for 1 min, and 68 °C for 2 min followed by 7 min at 68 °C in the last cycle for elongation. Purification of DNA fragments and nucleotide sequence determination were performed as described previously (Iwai et al., 2006).

2.4. Phylogenetic analysis and calculation of pairwise genetic distances

For phylogenetic analysis, the nucleotide sequences (positions 623–1012; 390 bp) and deduced amino acid sequences (130 aa) of the partial HRV *VP4/VP2* coding region were analyzed phylogenetically with the CLUSTAL W program available on the DNA Data Bank of Japan homepage (http://www.ddbj.nig.ac.jp/index-j.html) and TreeView (version 1.6.6; http://taxonomy.zoology.gla.ac.uk/rod/treeview.html). Evolutionary distances were estimated according to the Kimura's 2-parameter method, and the phylogenetic tree was constructed with the neighbor-joining method (Kimura, 1980; Saitou and Nei, 1987). The reliability of the tree was estimated with 1000 bootstrap replications. Genetic distances among reference (representative) strains may be important in phylogenetic analysis. Thus, to construct the phylogenetic tree, we preferably selected the reference strains having constant genetic distances (interspecies distances, 0.237 ± 0.030), and used the following as references strains in this study: HRV1B, HRV7, HRV8, HRV9, HRV12, HRV15, HRV16, HRV19, HRV28, HRV29, HRV47, HRV49, HRV55, HRV56, HRV60, and HRV63. In addition, some human rhinovirus species B (HRV-B), human rhinovirus species C (HRV-C) and human enterovirus species D (HEV-D) were used as reference strains as previously described (Piralla et al., 2009). Echovirus 11(Echo-11), which belongs to the human enterovirus species B was used as the outgroup (Piralla et al., 2009). In order to assess interspecies frequency distributions and the frequency distribution of each intercluster of HRV-A, we calculated pairwise genetic distances for all of the strains, including the present isolates and reference strains, as previously described (Katayama et al., 2002).

3. Results

3.1. Phylogenetic and cluster analysis

Phylogenetic trees based on the nucleotide sequences (390 nt) and the deduced amino acid sequences (130 aa) of the *VP4/VP2* coding region, including the present strains ($n = 76$) and representative reference strains ($n = 16$) belonging to HRV-A, are shown in Fig. 1a and b, respectively. In addition, we show the corresponding phylogenetic trees for the representative reference strains alone (Fig. 1c and d, respectively). Phylogenetic trees based on the nucleotide and deduced amino acid sequences for the present and reference strains of HRV-A species could be classified into 11 and 8 clusters, respectively. At the nucleotide level, the homology among the present strains ranged from 66.6% to 100%, while at the deduced amino acid level the homology ranged from 84.7% to 100%. On the phylogenetic tree based on the nucleotide sequences, the numbers of the present strains in each cluster were as follows: Cluster 1, 6 strains; Cluster 2, 8 strains; Cluster 3, 7 strains; Cluster 4, 8 strains; Cluster 5, 10 strains; Cluster 6, 7 strains; Cluster 7, 4 strains; Cluster 8, 4 strains; Cluster 9, 6 strains; Cluster 10, 10 strain; and Cluster 11, 6 strains. On the phylogenetic tree based on the deduced amino acid sequences, the numbers of the present strains in each cluster were as follows: Cluster 1, 20 strains; Cluster 2, 9 strains; Cluster 3, 10 strains; Cluster 4, 1 strain; Cluster 5, 11 strains; Cluster 6, 4 strains; Cluster 7, 19 strains; and Cluster 8, 2 strains. Notably, on the phylogenetic tree based on nucleotide sequences, Clusters 2, 3, 5 and 9 were associated with both URI and wheezy bronchiolitis, whereas other strains were associated with URI alone. As well, on the phylogenetic tree based on amino acid sequences, Clusters 3, 7, and 8 were associated with both URI and wheezy bronchiolitis. These results suggest that the present HRV-A strains which had a wide nucleotide divergence (66.6–100% homology) were circulating in the Yamagata area during the investigation period.

Table 1
Patients' data, HRV strain, and cluster.

Patient	Age (year)	Sampling date	Disease	Strain	Cluster	GenBank accession no.
1	16	23 January, 2003	URI*	HRVi/Yamagata.JPN/4.03	8**, 1***	AB474093
2	3	25 March, 2003	URI	HRVi/Yamagata.JPN/13.03	3, 5	AB474094
3	15	18 April, 2003	URI	HRVi/Yamagata.JPN/16.03	5, 3	AB474095
4	7	18 April, 2003	URI	HRVi/Yamagata.JPN/16-2.03	1, 7	AB474096
5	11	30 April, 2003	URI	HRVi/Yamagata.JPN/18.03	9, 2	AB474100
6	9	30 April, 2003	URI	HRVi/Yamagata.JPN/18-2.03	3, 5	AB474101
7	5	7 May, 2003	URI	HRVi/Yamagata.JPN/19.03	11, 6	AB474102
8	7	12 May, 2003	URI	HRVi/Yamagata.JPN/20.03	10, 6	AB474103
9	1	10 May, 2003	URI	HRVi/Yamagata.JPN/19-2.03	6, 1	AB474104
10	1	12 May, 2003	URI	HRVi/Yamagata.JPN/20-2.03	11, 2	AB474105
11	0	9 September, 2003	URI	HRVi/Yamagata.JPN/37.03	3, 5	AB474106
12	4	20 September, 2003	Wheezy bronchiolitis	HRVi/Yamagata.JPN/38.03	9, 8	AB474107
13	2	22 September, 2003	Wheezy bronchiolitis	HRVi/Yamagata.JPN/39.03	2, 7	AB474108
14	2	30 September, 2003	URI	HRVi/Yamagata.JPN/40.03	10, 1	AB474109
15	6	6 October, 2003	URI	HRVi/Yamagata.JPN/41.03	3, 7	AB475008
16	0	10 October, 2003	URI	HRVi/Yamagata.JPN/41-2.03	3, 7	AB474110
17	0	10 October, 2003	LRI	HRVi/Yamagata.JPN/41-3.03	8, 1	AB474111
18	9	20 October, 2003	URI	HRVi/Yamagata.JPN/43.03	3, 7	AB474112
19	0	12 November, 2003	Wheezy bronchiolitis	HRVi/Yamagata.JPN/46.03	3, 7	AB475009
20	6	17 November, 2003	URI	HRVi/Yamagata.JPN/47.03	10, 2	AB474113
21	2	19 November, 2003	URI	HRVi/Yamagata.JPN/47-2.03	9, 8	AB474114
22	11	20 November, 2003	URI	HRVi/Yamagata.JPN/47-3.03	10, 2	AB474115
23	8	21 November, 2003	URI	HRVi/Yamagata.JPN/47-4.03	4, 5	AB474116
24	1	16 December, 2003	Wheezy bronchiolitis	HRVi/Yamagata.JPN/51.03	5, 3	AB474117
25	2	17 December, 2003	URI	HRVi/Yamagata.JPN/51-2.03	10, 1	AB474118
26	7	21 January, 2004	URI	HRVi/Yamagata.JPN/4.04	5, 3	AB474119
27	13	30 March, 2004	URI	HRVi/Yamagata.JPN/14.04	2, 7	AB474120
28	3	26 April, 2004	URI	HRVi/Yamagata.JPN/18.04	2, 7	AB474121
29	7	26 April, 2004	URI	HRVi/Yamagata.JPN/18-2.04	5, 3	AB474122
30	2	7 May, 2004	URI	HRVi/Yamagata.JPN/19.04	10, 1	AB474123
31	10	2 June, 2004	URI	HRVi/Yamagata.JPN/23.04	2, 7	AB474124
32	0	28 July, 2004	URI	HRVi/Yamagata.JPN/31.04	6, 1	AB474125
33	0	16 August, 2004	URI	HRVi/Yamagata.JPN/34.04	4, 5	AB474126
34	1	14 September, 2004	URI	HRVi/Yamagata.JPN/38.04	4, 5	AB474127
35	2	2 November, 2004	URI	HRVi/Yamagata.JPN/45.04	6, 1	AB474128
36	4	20 April, 2005	URI	HRVi/Yamagata.JPN/16.05	6, 1	AB474129
37	1	12 May, 2005	URI	HRVi/Yamagata.JPN/19.05	6, 1	AB474130
38	2	16 May, 2005	URI	HRVi/Yamagata.JPN/20.05	9, 1	AB474131
39	3	24 May, 2005	URI	HRVi/Yamagata.JPN/21.05	9, 1	AB474132
40	6	13 October, 2005	URI	HRVi/Yamagata.JPN/41.05	11, 2	AB474133
41	11	18 October, 2005	URI	HRVi/Yamagata.JPN/42.05	11, 2	AB474134
42	4	28 February, 2006	URI	HRVi/Yamagata.JPN/9.06	5, 3	AB474135
43	10	18 March, 2006	URI	HRVi/Yamagata.JPN/11.06	10, 1	AB474136
44	9	24 April, 2006	URI	HRVi/Yamagata.JPN/17.06	5, 3	AB474137
45	1	1 May, 2006	URI	HRVi/Yamagata.JPN/18.06	10, 6	AB474138
46	3	19 May, 2006	URI	HRVi/Yamagata.JPN/20.06	2, 7	AB474139
47	0	27 May, 2006	Wheezy bronchiolitis	HRVi/Yamagata.JPN/21.06	2, 7	AB474140
48	1	26 May, 2006	URI	HRVi/Yamagata.JPN/21-2.06	5, 3	AB474141
49	8	31 May, 2006	URI	HRVi/Yamagata.JPN/22.06	5, 3	AB474142
50	0	6 June, 2006	URI	HRVi/Yamagata.JPN/23.06	4, 7	AB474143
51	1	6 June, 2006	Wheezy bronchiolitis	HRVi/Yamagata.JPN/23-2.06	2, 7	AB474144
52	1	21 June, 2006	URI	HRVi/Yamagata.JPN/25.06	7, 1	AB474145
53	1	21 June, 2006	URI	HRVi/Yamagata.JPN/25-2.06	8, 2	AB474146
54	2	21 July, 2006	URI	HRVi/Yamagata.JPN/29.06	2, 7	AB474148
55	0	1 December, 2006	URI	HRVi/Yamagata.JPN/48-2.06	8, 1	AB474150
56	1	30 March, 2007	URI	HRVi/Yamagata.JPN/13.07	7, 1	AB474151
57	1	23 May, 2007	URI	HRVi/Yamagata.JPN/21.07	4, 5	AB474152
58	3	2 June, 2007	URI	HRVi/Yamagata.JPN/22.07	1, 8	AB474153
59	3	6 June, 2007	URI	HRVi/Yamagata.JPN/23.07	10, 6	AB474154
60	1	27 June, 2007	URI	HRVi/Yamagata.JPN/26.07	1, 7	AB474155
61	6	22 June, 2007	URI	HRVi/Yamagata.JPN/25.07	1, 7	AB474156
62	2	22 June, 2007	URI	HRVi/Yamagata.JPN/25-2.07	1, 7	AB474157
63	2	3 July, 2007	URI	HRVi/Yamagata.JPN/27.07	4, 5	AB474158
64	10	13 July, 2007	URI	HRVi/Yamagata.JPN/28.07	1, 7	AB474159
65	5	21 August, 2007	URI	HRVi/Yamagata.JPN/34.07	5, 3	AB474160
66	8	25 September, 2007	URI	HRVi/Yamagata.JPN/39.07	9, 4	AB474161
67	0	29 September, 2007	URI	HRVi/Yamagata.JPN/35.07	6, 1	AB474163
68	1	3 October, 2007	URI	HRVi/Yamagata.JPN/40-2.07	5, 3	AB474164
69	2	9 October, 2007	URI	HRVi/Yamagata.JPN/41.07	4, 5	AB474165
70	1	15 October, 2007	URI	HRVi/Yamagata.JPN/42.07	4, 5	AB474166
71	2	18 October, 2007	URI	HRVi/Yamagata.JPN/42-2.07	7, 1	AB474167
72	0	24 October, 2007	URI	HRVi/Yamagata.JPN/43.07	11, 2	AB474168
73	1	1 November, 2007	URI	HRVi/Yamagata.JPN/44.07	6, 1	AB474169
74	0	6 November, 2007	URI	HRVi/Yamagata.JPN/45.07	7, 1	AB474170
75	1	6 November, 2007	URI	HRVi/Yamagata.JPN/45-2.07	11, 2	AB474171
76	2	22 November, 2007	URI	HRVi/Yamagata.JPN/47.07	10, 5	AB474172

* URI: upper respiratory infection.
** Left number: cluster numbers as phylogenetic tree based on the nucleotide sequences.
*** Right number: cluster numbers as phylogenetic tree based on the amino acid sequences.

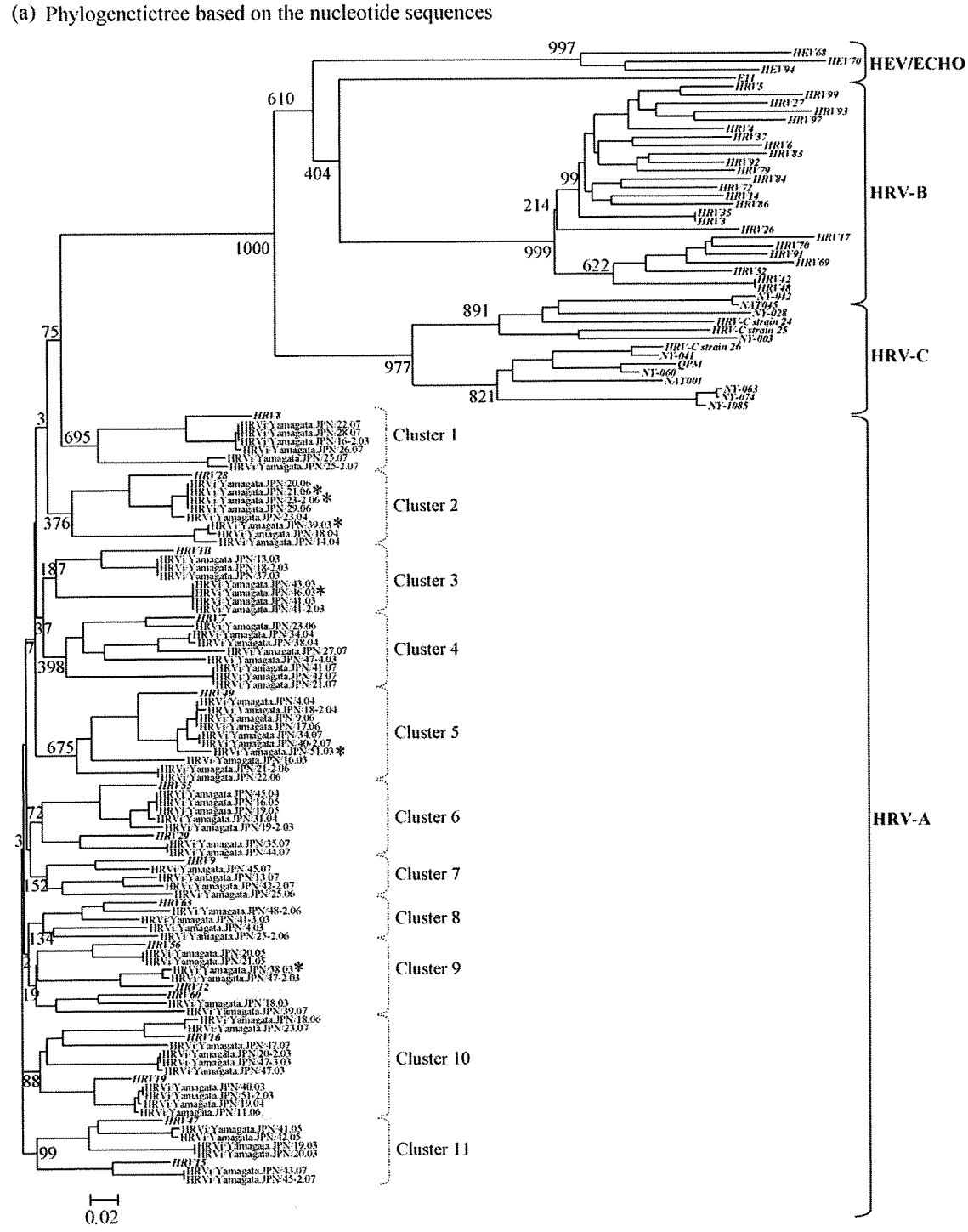

Fig. 1. Phylogenetic tree based on the *VP4/VP2* coding region of human rhinovirus species A (HRV-A), human rhinovirus species B (HRV-B), human rhinovirus species C (HRV-C), and human enterovirus species D (HEV-D). Echovirus 11(Echo-11), which belongs to the human enterovirus species B, was used as an outgroup. (a) Phylogenetic tree based on nucleotide sequences of the *VP4/VP2* coding region (390 nt) including the present strains (76 strains) and representative reference strains (16 strains). (b) Phylogenetic tree based on deduced amino acid sequences of the *VP4/VP2* coding region (130 aa) including the present strains and representative reference strains. Distance was calculated according to Kimura's 2-parameter method, and the tree was plotted with the neighbor-joining method. Numbers at each branch indicate the bootstrap values of the clusters supported by that branch. Reference strains are shown in bold type. (c and d) Phylogenetic trees based nucleotide sequences and amino acid sequences of the corresponding region for representative reference strains. GenBank accession numbers of references strains are as follows: HRV1B (GenBank accession no. D00239), HRV7 (AF343589), HRV8 (D00239), HRV9 (AF343605), HRV12 (AY016405), HRV15 (AF343630), HRV16 (L24917), HRV19 (AF343632) HRV28 (DQ473508), HRV29 (AF343615), HRV47 (FJ445133), HRV49 (AF343598), HRV55 (AF343621), HRV56 (FJ445140), HRV60 (AF343627), HRV63 (FJ445146), HRV3 (EF173422), HRV4 (AF343655), HRV5 (AF343651), HRV6 (DQ473486), HRV14 (K02121), HRV17 (AF343645), HRV26 (AF343653), HRV27 (AF343654), HRV35 (FJ445187), HRV37 (EF173423), HRV42 (FJ445130), HRV48 (DQ473488), HRV52 (FJ445188), HRV69 (FJ445151), HRV70 (AF343646), HRV72 (AF343650), HRV79 (FJ445155), HRV83 (AF343647), HRV84 (FJ445162), HRV86 (AF343648), HRV91 (FJ445168), HRV92 (FJ445169), HRV93 (EF173425), HRV97 (FJ445172), HRV99 (AF343652), HRV-C strain 24 (EF582385), HRV-C strain 25 (EF582386), HRV-C strain 26 (EF582387), QPM (EF186077), NY-003 (DQ875929), NY-028 (DQ875931), NY-041 (DQ875921), NY-042 (DQ875926), NY-060 (DQ875928), NY-063 (DQ875924), NY-074 (DQ875932), NY-1085 (DQ875925), NAT001 (FF077279), NAT045 (EF077280), HEV68 (EF107098), HEV70 (EV70CG), HEV94 (DQ916376), and Echo-11 (EU167522). *Strains from wheezy bronchiolitis.

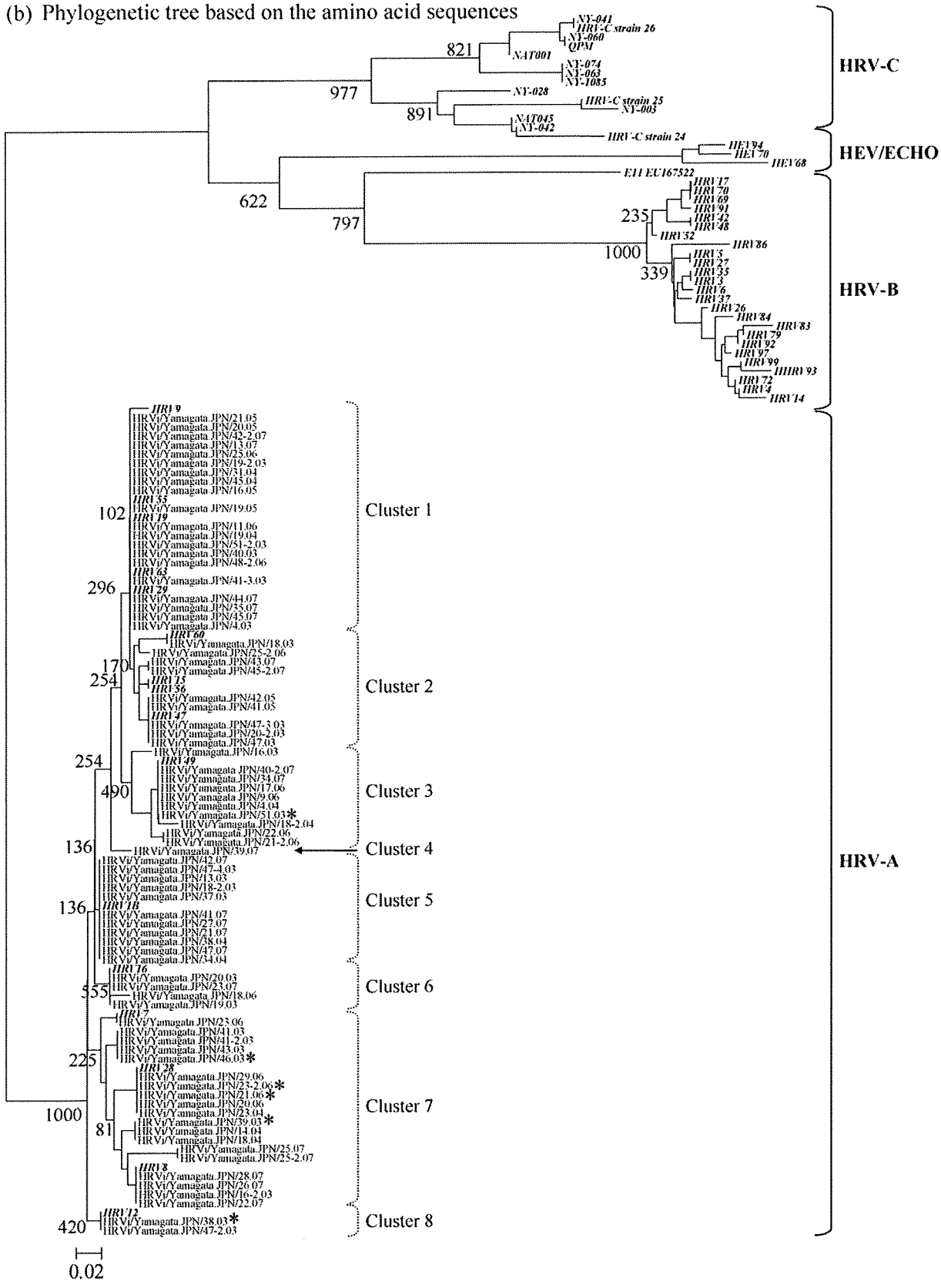

Fig. 1. (*Continued*)

(c) Phylogenetic tree based on the nucleotide sequences (reference strains)

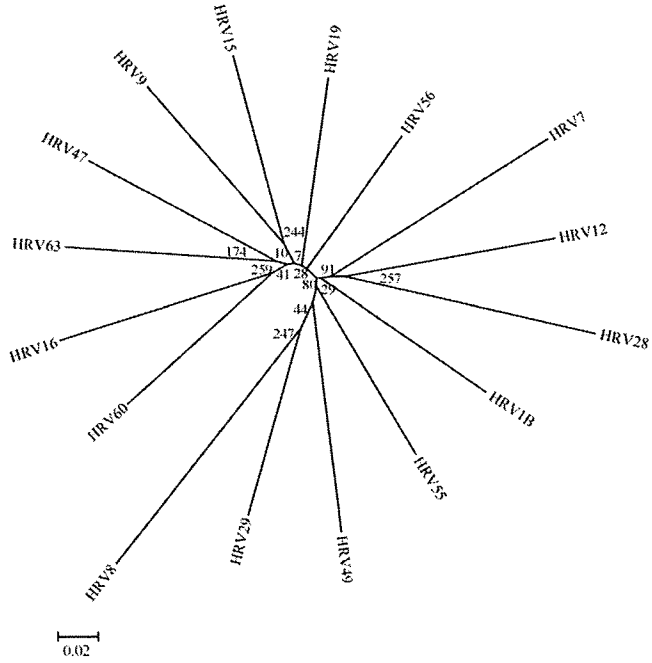

(d) Phylogenetic tree based on the amino acid sequences (reference strains)

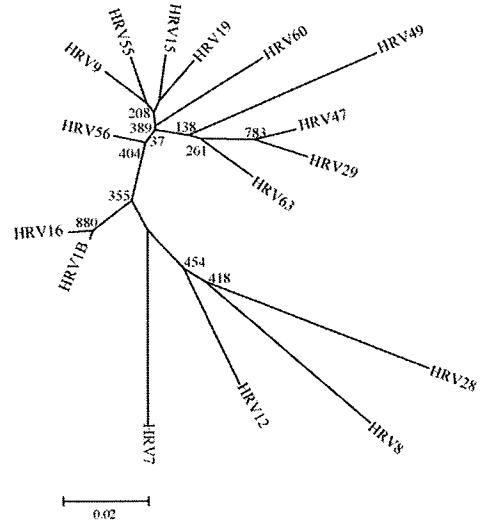

Fig. 1. (*Continued*).

3.2. Distribution of pairwise distances of interspecies of HRV-A based on the nucleotide and amino acid sequences

We calculated interspecies distances of HRV-A by the distribution of pairwise distances (Figs. 2a–k and 3a–i). Among the present and reference strains, the interspecies distances based on the nucleotide and amino acid sequences were 0.235 ± 0.048 and 0.076 ± 0.033 (mean ± SD), respectively (Figs. 2a, 3a). The intercluster distances based on the nucleotide sequences were as follows: Cluster 1, 0.136 ± 0.101 (mean ± SD, Fig. 2b); Cluster 2, 0.115 ± 0.086 (c); Cluster 3, 0.152 ± 0.115 (d); Cluster 4, 0.142 ± 0.062 (e); Cluster 5, 0.085 ± 0.058 (f); Cluster 6, 0.130 ± 0.093 (g); Cluster 7, 0.159 ± 0.053 (h); Cluster 8, 0.167 ± 0.053 (i); Cluster 9, 0.184 ± 0.064 (j); Cluster 10, 0.169 ± 0.072 (k) and Cluster 11, 0.153 ± 0.072 (l). Next, the intercluster distances based on the amino acid sequences were as follows: Cluster 1, 0.031 ± 0.020 (mean ± SD, Fig. 3b); Cluster 2, 0.040 ± 0.016 (c); Cluster 3, 0.012 ± 0.012 (d); Cluster 5, 0.030 ± 0.025 (e); Cluster 6, 0.027 ± 0.020 (f); Cluster 7, 0.079 ± 0.041 (g); and Cluster 8, 0 (h). The longest pairwise intercluster distances based on the nucleotide and amino acid sequences were Cluster 9 and Cluster 7, respectively, whereas the shortest pairwise distances were Cluster 5 and Cluster 8, respectively.

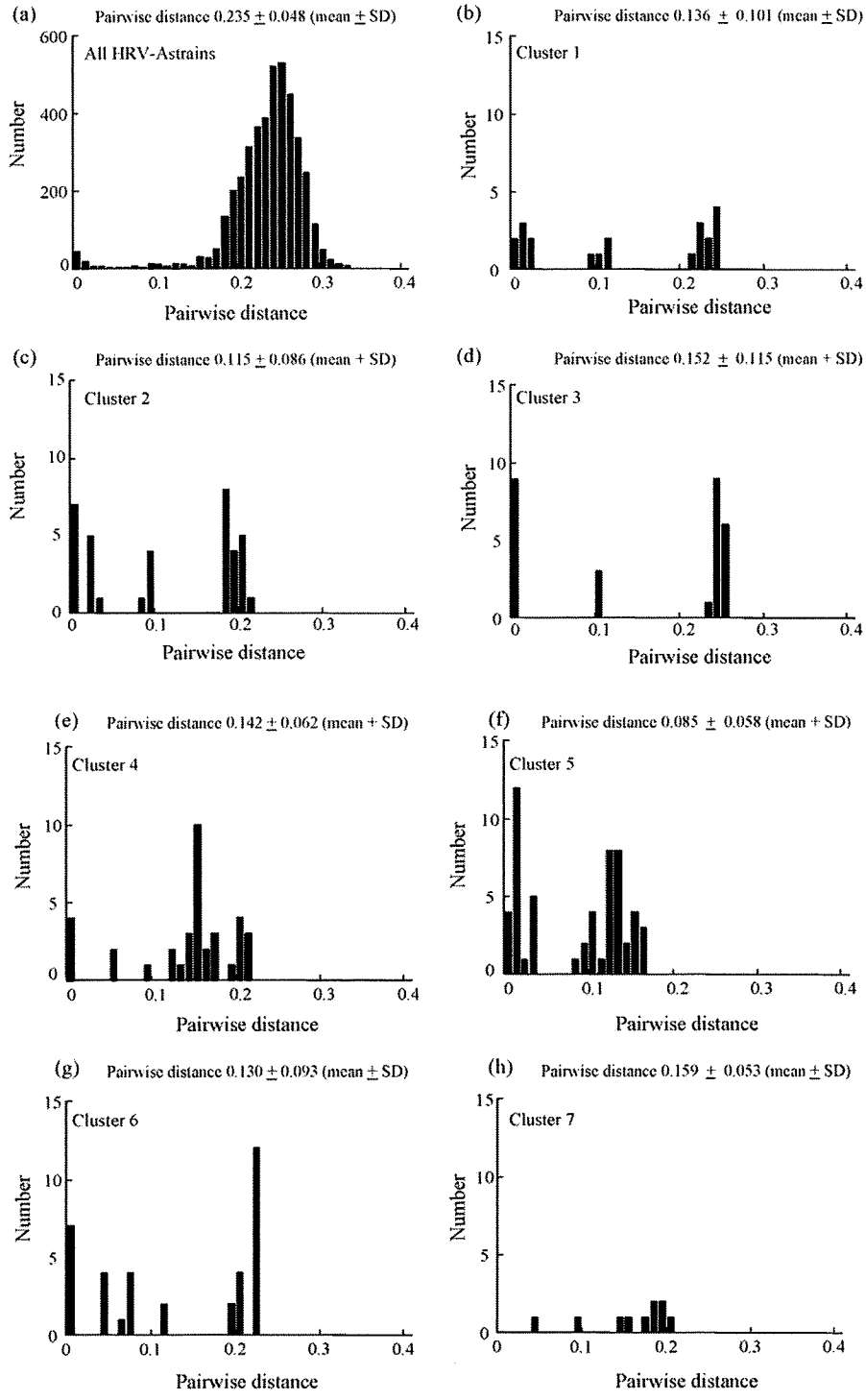

Fig. 2. Distributions of pairwise interspecies distances and pairwise distances for each intercluster for HRV-A based on nucleotide sequences of *VP4/VP2* coding region (390 nt). (a) Distribution of pairwise interspecies distances based on nucleotide sequences of the *VP4/VP2* coding region. (b–l) Distributions of pairwise distances for each intercluster (Clusters 1–11).

4. Discussion

To ascertain the address molecular epidemiology of domestic HRV-A infection, we performed phylogenetic and cluster analysis of the *VP4/VP2* coding region of prevalent strains (76 isolates) isolated from children with ARI in Yamagata prefecture, Japan during the period 2003–2007. Phylogenetic analysis based on the nucleotide and deduced amino acid sequences showed that the present HRV-A strains were clearly classified into 11 and 8 clusters, respectively. These viruses showed more than 30% of nucleotide divergence of the *VP4/VP2* cording region. The findings suggest that HRV-A with a wide genetic divergence was associated with URI and wheezy bronchiolitis during the investigation period in the study area.

Matsumoto et al. (1991) reported that approximately 32% of Japanese patients with ARI had associated HRV, although viruses were confirmed by a physicochemical method. Another study

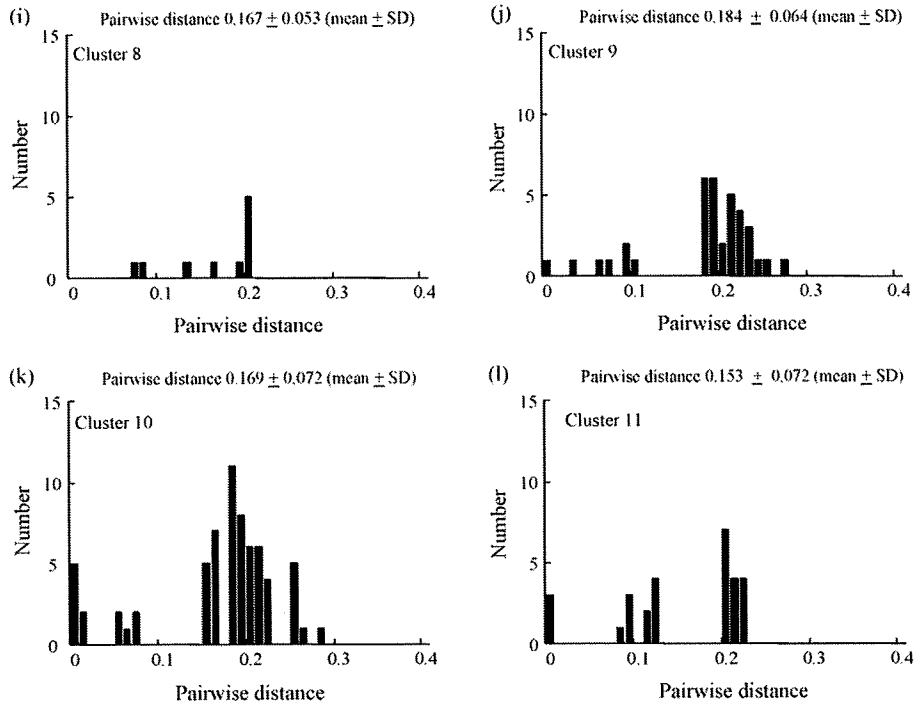

Fig. 2. (*Continued*).

found HRV in hospitalized infants with bronchiolitis and wheezing (Jartti et al., 2009). Calvo et al. (2007) reported that 25% of hospitalized infants with ARI had HRV infection as confirmed by multiplex PCR. In addition, HRV infections are frequently found in patients hospitalized with pneumonia (Cheuk et al., 2007). Savolainen et al. (2002a) showed that some serotypes of HRV, including HRV45, 78, and 81, were frequently associated with ARI in Finland. In American children with wheezing, various serotypes of HRV, including HRV30, 44, and 49, were found (Khetsuriani et al., 2008). In the present study, approximately 90% of patients with ARI had URI, and approximately 10% had wheezy bronchiolitis. Recent studies have shown that HRV can be classified into several species (Savolainen et al., 2002a,b). Savolainen et al. (2002b) reported that 61 isolates from patients with ARI could be classified into genetic groups 1 and 2, and these genetic groups could be further categorized into 12 clusters. Relations between genetic and serologic HRV type have been studied (Savolainen et al., 2002a). Most prototype HRV strains (isolates) have been classified into 2 species (HRV-A and -B). Of them, viruses belonging to species HRV-A comprise the major agent associated with ARI (Savolainen et al., 2002a). HRV-A can be subclassified into various clusters (Savolainen et al., 2002a). For example, McErlean reported that frequently detected HRV strains can be classified into 3 genotypes (Types A1, A2, and B) (McErlean et al., 2007). However, the detailed molecular epidemiology of HRV is not known. Moreover, to the best of our knowledge, there have been few molecular epidemiologic studies of HRV-A in Asian countries including Japan. Therefore, we performed a detailed phylogenetic and cluster analysis of HRV-A of patients with ARI, such as upper respiratory infections and wheezy bronchiolitis, in Yamagata prefecture, Japan. We found that prevalent HRV-A strains isolated from Japanese patients with ARI showed a wide nucleotide divergence. The data suggested that HRV-A strains belonging to some clusters were associated with wheezy bronchiolitis. However, we do not know whether these viruses can easily cause wheezy bronchiolitis because only 6 cases of wheezy bronchiolitis caused by HRV-A were examined in the present study. Recent evidence suggests that some genotypes of respiratory viruses, such as HRV, respiratory syncytial virus (RSV), and parainfluenza viruses, may be linked to virus-induced asthma (Jartti et al., 2004, 2007; Martinello et al., 2002). For example, a specific genotype (GA 3) of RSV may be associated with significantly greater severity of illness (Martinello et al., 2002). However, another report showed no association between severity of illness and RSV subgroups, and the severity was instead associated with the amount of RSV in nasopharyngial aspirates (Campanini et al., 2007; Sato et al., 2005). Thus, the association between a specific virus type and the severity of RSV infections, including bronchiolitis, has not been precisely addressed. In addition, Johnston (2007) reported that HRV infection is strongly related to virus-induced asthma or exacerbation of asthma. As possible reason for this association with HRV-induced asthma is insufficient production of the cytokine interferon-β or λ; however, the molecular mechanisms underlying this are not fully understood as yet (Johnston, 2007). Additional studies with large numbers of patients with HRV-induced airway hyperresponsiveness, including asthma, would be beneficial.

The *VP4/VP2* coding region encodes interior viral capsid. Genetic clustering on the basis of the *VP4/VP2* sequences was reported to be an effective method for the identification of many types of HRV isolates (Savolainen et al., 2002a). To better perform phylogenetic and cluster analysis of many types of HRV-A in the present study, we selected the *VP4/VP2* coding region, which resulted in the construction of a clearly distinguishable phylogenetic tree (Savolainen et al., 2002a; Kiang et al., 2007). Thus, the use of this coding region for phylogenetic analysis of HRV may be suitable for the clustering of many field isolates of HRV, consistent with earlier reports (Savolainen et al., 2002a,b).

We were able to collect clinical specimens from only a relatively small number of pediatric patients with ARI in a limited area (Yamagata prefecture), covering only a small number of HRV-A strains from children who attended a pediatric clinic. In addition, no seasonal variation of HRV was found in the present data, but it may be important to address seasonal variation regarding HRV epidemiology as a future research topic. To address the

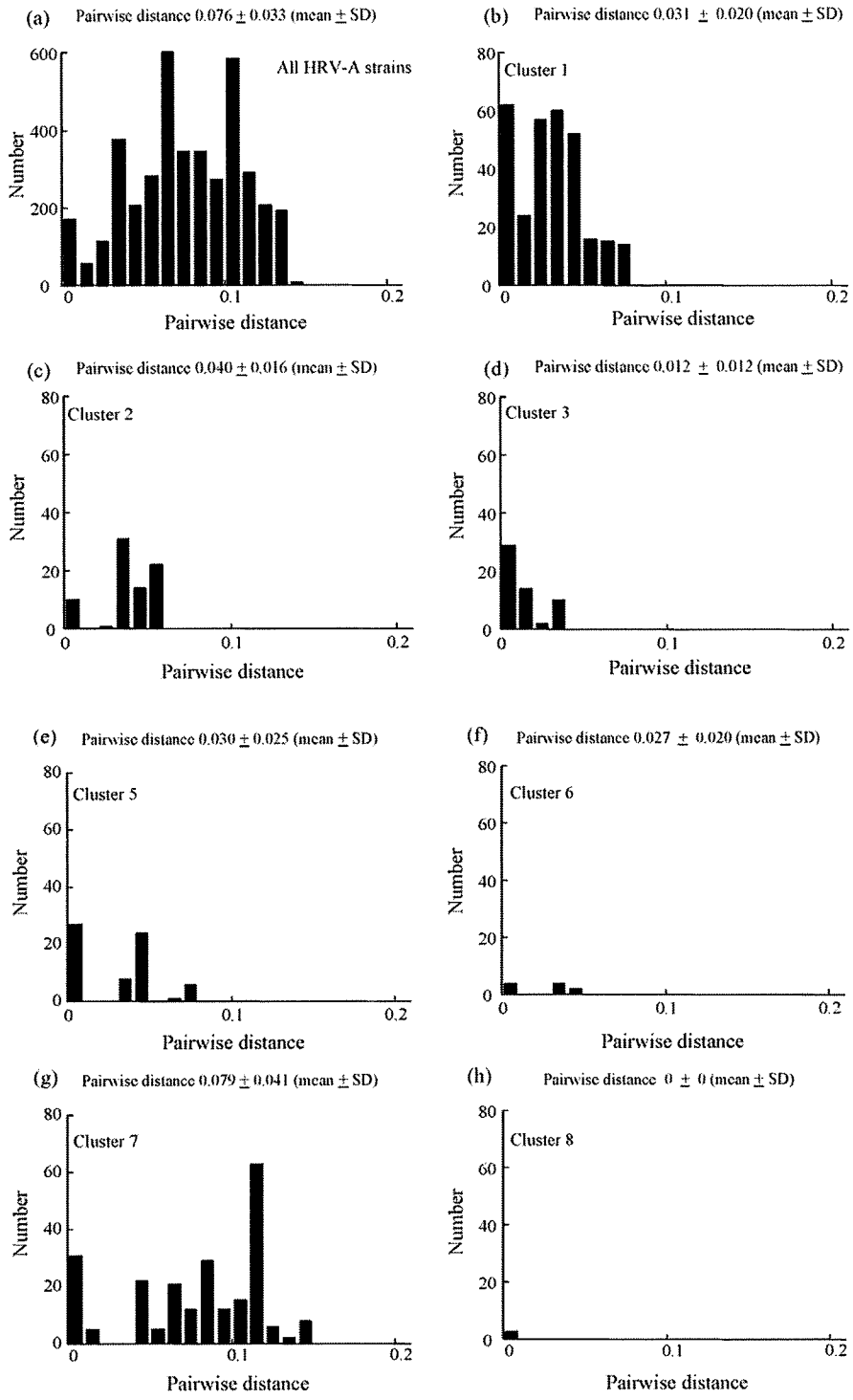

Fig. 3. Distributions of pairwise interspecies distances and pairwise distances for each intercluster for HRV-A based on deduced amino acid sequences of *VP4/VP2* coding region (130 aa). (a) Distribution of pairwise interspecies distances based on amino acid sequences of the *VP4/VP2* coding region. (b–h) Distributions of pairwise distances for each intercluster (Clusters 1–3 and 5–8).

domestic epidemiology of HRV more comprehensively large numbers of HRV strains derived from adults and large areas will be required.

In conclusion, various genetic types of HRV-A appear to be associated with ARI, including URI and wheezy bronchiolitis, in Japanese children. Further molecular epidemiologic investigations regarding the other HRV species (HRV-B and HRV-C) should be performed.

Acknowledgements

We thank Drs. Kazushi Motomura and Hironori Sato (Center for Pathogen Genomics, National Institute of Infectious Diseases, Japan) for helpful discussions. This work was supported in part by Research on Emerging and Re-emerging Infectious Diseases, Labour, and Welfare Programs from the Ministry of Health, Labour, and Welfare, Japan (No. 24-19211301).

References

Campanini, G., Percivalle, E., Baldanti, F., Rovida, F., Bertaina, A., Marchi, A., Stronati, M., Gerna, G., 2007. Human respiratory syncytial virus (hRSV) RNA quantification in nasopharyngeal secretions identifies the hRSV etiologic role in acute respiratory tract infections of hospitalized infants. J. Clin. Virol. 39, 119–124.

Calvo, C., García-García, M.L., Blanco, C., Pozo, F., Flecha, I.C., Pérez-Breña, P., 2007. Role of rhinovirus in hospitalized infants with respiratory tract infections in Spain. Pediatr. Infect. Dis. J. 26, 904–908.

Cherry, J.D., 2003. The Common Cold. In: Feigin, R.D., Cherry, J.D., Demmler, G.J., Kaplan, S.L. (Eds.), Textbook of Pediatric Infectious Diseases, fifth ed. Saunders, Philadelphia, pp. 140–146.

Cheuk, D.K., Tang, I.W., Chan, K.H., Woo, P.C., Peiris, M.J., Chiu, S.S., 2007. Rhinovirus infection in hospitalized children in Hong Kong: a prospective study. Pediatr. Infect. Dis. J. 26, 995–1000.

Imakita, M., Shiraki, K., Yutani, C., Ishibashi-Ueda, H., 2000. Pneumonia caused by rhinovirus. Clin. Infect. Dis. 30, 611–612.

Iwai, M., Yoshida, H., Matsuura, K., Fujimoto, T., Shimizu, H., Takizawa, T., Nagai, Y., 2006. Molecular epidemiology of echoviruses 11 and 13, based on an environmental surveillance conducted in Toyama Prefecture, 2002–2003. Appl. Environ. Microbiol. 72, 6381–6387.

Jackson, D.J., Gangnon, R.E., Evans, M.D., Roberg, K.A., Anderson, E.L., Pappas, T.E., Printz, M.C., Lee, W.M., Shult, P.A., Reisdorf, E., Carlson-Dakes, K.T., Salazar, L.P., DaSilva, D.F., Tisler, C.J., Gern, J.E., Lemanske Jr., R.F., 2008. Wheezing rhinovirus illnesses in early life predict asthma development in high-risk children. Am. J. Respir. Crit. Care Med. 178, 667–672.

Jartti, T., Lehtinen, P., Vuorinen, T., Osterback, R., van den Hoogen, B., Osterhaus, A.D., Ruuskanen, O., 2004. Respiratory picornaviruses and respiratory syncytial virus as causative agents of acute expiratory wheezing in children. Emerg. Infect. Dis. 10, 1095–1101.

Jartti, T., Lehtinen, P., Vuorinen, T., Ruuskanen, O., 2009. Bronchiolitis: age and previous wheezing episodes are linked to viral etiology and atopic characteristics. Pediatr. Infect. Dis. J. 28, 311–317.

Jartti, T., Waris, M., Niesters, H.G., Allander, T., Ruuskanen, O., 2007. Respiratory viruses and acute asthma in children. J. Allergy Clin. Immunol. 120, 216.

Johnston, S.L., 2007. Innate immunity in the pathogenesis of virus-induced asthma exacerbations. Proc. Am. Thorac. Soc. 4, 267–270.

Johnston, S.L., Pattemore, P.K., Sanderson, G., Smith, S., Campbell, M.J., Josephs, L.K., Cunningham, A., Robinson, B.S., Myint, S.H., Ward, M.E., Tyrrell, D.A., Holgate, S.T., 1996. The relationship between upper respiratory infections and hospital admissions for asthma: a time-trend analysis. Am. J. Respir. Crit. Care Med. 154, 654–660.

Katayama, K., Shirato-Horikoshi, H., Kojima, S., Kageyama, T., Oka, T., Hoshino, F., Fukushi, S., Shinohara, M., Uchida, K., Suzuki, Y., Gojobori, T., Takeda, N., 2002. Phylogenetic analysis of the complete genome of 18 Norwalk-like viruses. Virology 299, 225–239.

Khetsuriani, N., Lu, X., Teague, W.G., Kazerouni, N., Anderson, L.J., Erdman, D.D., 2008. Novel human rhinoviruses and exacerbation of asthma in children. Emerg. Infect. Dis. 14, 1793–1796.

Kiang, D., Yagi, S., Kantardjieff, K.A., Kim, E.J., Louie, J.K., Schnurr, D.P., 2007. Molecular characterization of a variant rhinovirus from an outbreak associated with uncommonly high mortality. J. Clin. Virol. 38, 227–237.

Kimura, M., 1980. A simple method for estimating evolutionary rates of base substitutions through comparative studies of nucleotide sequences. J. Mol. Evol. 16, 111–120.

Lau, S.K., Yip, C.C., Tsoi, H.W., Lee, R.A., So, L.Y., Lau, Y.L., Chan, K.H., Woo, P.C., Yuen, K.Y., 2007. Clinical features and complete genome characterization of a distinct human rhinovirus (HRV) genetic cluster, probably representing a previously undetected HRV species, HRV-C, associated with acute respiratory illness in children. J. Clin. Microbiol. 45, 3655–3664.

Martinello, R.A., Chen, M.D., Weibel, C., Kahn, J.S., 2002. Correlation between respiratory syncytial virus genotype and severity of illness. J. Infect. Dis. 186, 839–842.

Matsumoto, I., Yoshida, S., Takahashi, K., Kawana, R., 1991. Virological surveillance of acute respiratory tract illnesses of children in Morioka, Japan. I. Epidemiological patterns of infection with respiratory viruses over a 10-year period. Kansenshogaku Zasshi 65, 423–432.

McErlean, P., Shackelton, L.A., Lambert, S.B., Nissen, M.D., Sloots, T.P., Mackay, I.M., 2007. Characterisation of a newly identified human rhinovirus, HRV-QPM, discovered in infants with bronchiolitis. J. Clin. Virol. 39, 67–75.

Mizuta, K., Abiko, C., Aoki, Y., Suto, A., Hoshina, H., Itagaki, T., Katsushima, N., Matsuzaki, Y., Hongo, S., Noda, M., Kimura, H., Ootani, K., 2008. Analysis of monthly isolation of respiratory viruses from children by cell culture using a microplate method: a two-year study from 2004 to 2005 in Yamagata, Japan. Jpn. J. Infect. Dis. 61, 196–201.

Nicholson, K.G., Kent, J., Ireland, D.C., 1993. Respiratory viruses and exacerbations of asthma in adults. BMJ 307, 982–986.

Papadopoulos, N.G., Moustaki, M., Tsolia, M., Bossios, A., Astra, E., Prezerakou, A., Gourgiotis, D., Kafetzis, D., 2002. Association of rhinovirus infection with increased disease severity in acute bronchiolitis. Am. J. Respir. Crit. Care Med. 165, 1285–1289.

Piralla, A., Rovida, F., Campanini, G., Rognoni, V., Marchi, A., Locatelli, F., Gerna, G., 2009. Clinical severity and molecular typing of human rhinovirus C strains during a fall outbreak affecting hospitalized patients. J. Clin. Virol. 45, 311–317.

Robert, C.W., 2003. Bronchiolitis and Infectious Asthma. In: Feigin, R.D., Cherry, J.D., Demmler, G.J., Kaplan, S.L. (Eds.), Textbook of Pediatric Infectious Diseases, fifth ed. Saunders, Philadelphia, pp. 273–282.

Saitou, N., Nei, M., 1987. The neighbor-joining method: a new method for reconstructing phylogenetic trees. Mol. Biol. Evol. 4, 406–425.

Sato, M., Saito, R., Sakai, T., Sano, Y., Nishikawa, M., Sasaki, A., Shobugawa, Y., Gejyo, F., Suzuki, H., 2005. Molecular epidemiology of respiratory syncytial virus infections among children with acute respiratory symptoms in a community over three seasons. J. Clin. Microbiol. 43, 36–40.

Savolainen, C., Blomqvist, S., Mulders, M.N., Hovi, T., 2002a. Genetic clustering of all 102 human rhinovirus prototype strains: serotype 87 is close to human enterovirus 70. J. Gen. Virol. 83, 333–340.

Savolainen, C., Mulders, M.N., Hovi, T., 2002b. Phylogenetic analysis of rhinovirus isolates collected during successive epidemic seasons. Virus Res. 85, 41–46.

Turner, R.B., Couch, R.B., 2007. Rhinovirus. In: Knipe, D.M., Hawley, P.M. (Eds.), Fields Virology, fifth ed. Lippincott Williams & Wilkins, Philadelphia, PA, pp. 895–909.

Wos, M., Sanak, M., Soja, J., Olechnowicz, H., Busse, W.W., Szczeklik, A., 2008. The presence of rhinovirus in lower airways of patients with bronchial asthma. Am. J. Respir. Crit. Care Med. 177, 1082–1089.

麻しんを疑ったら、検査診断にご協力を！

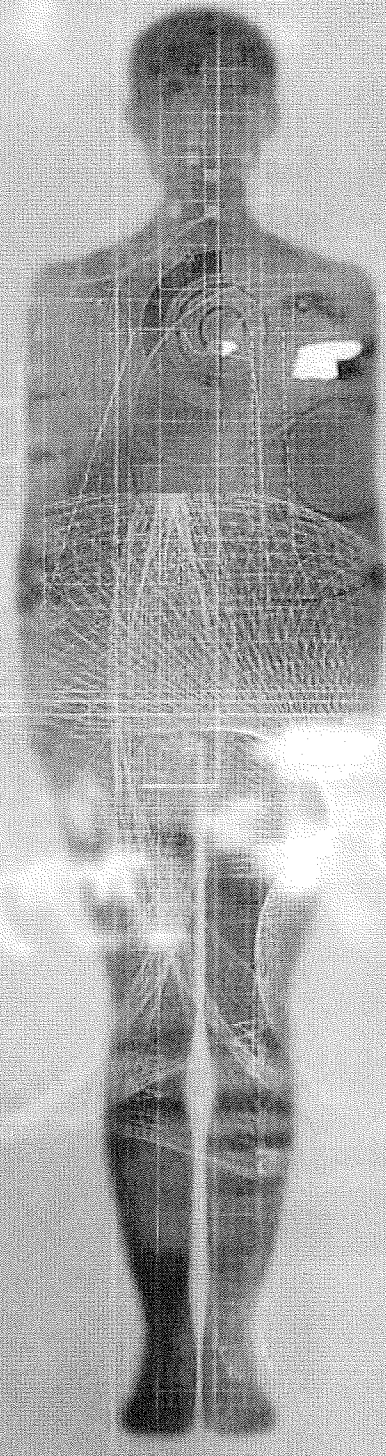

麻しんは全例、検査診断を！

麻しん患者は減少傾向にあります。目標達成まであともう少しです！

2009年第1～53週に届出された麻しん患者は741人（2010年1月7日現在報告数）であり、2008年の11,015人から大きく減少（93%減少）しました。
麻しん排除の目標は、輸入例を除いて1年間に人口100万人あたり1人未満になることですが、2009年は人口100万人あたり5.8人であり、目標まであと少しのところにきています。

「麻しんに関する特定感染症予防指針（2007年12月28日厚生労働省告示）」では、患者数が一定数以下になった場合、原則としてすべての患者について、検査診断することとしています。

1 に示したように、2009年の報告例741人のうち、検査診断例は438人（うち、修飾麻疹193人）で、全体の約60%となっています。

1 都道府県別病型別麻しん累積報告数 2009年第1週～53週（n=741）

Cumulative measles cases by prefecture and methods of diagnosis from week 1 to week 53, 2009 (as of January 7)

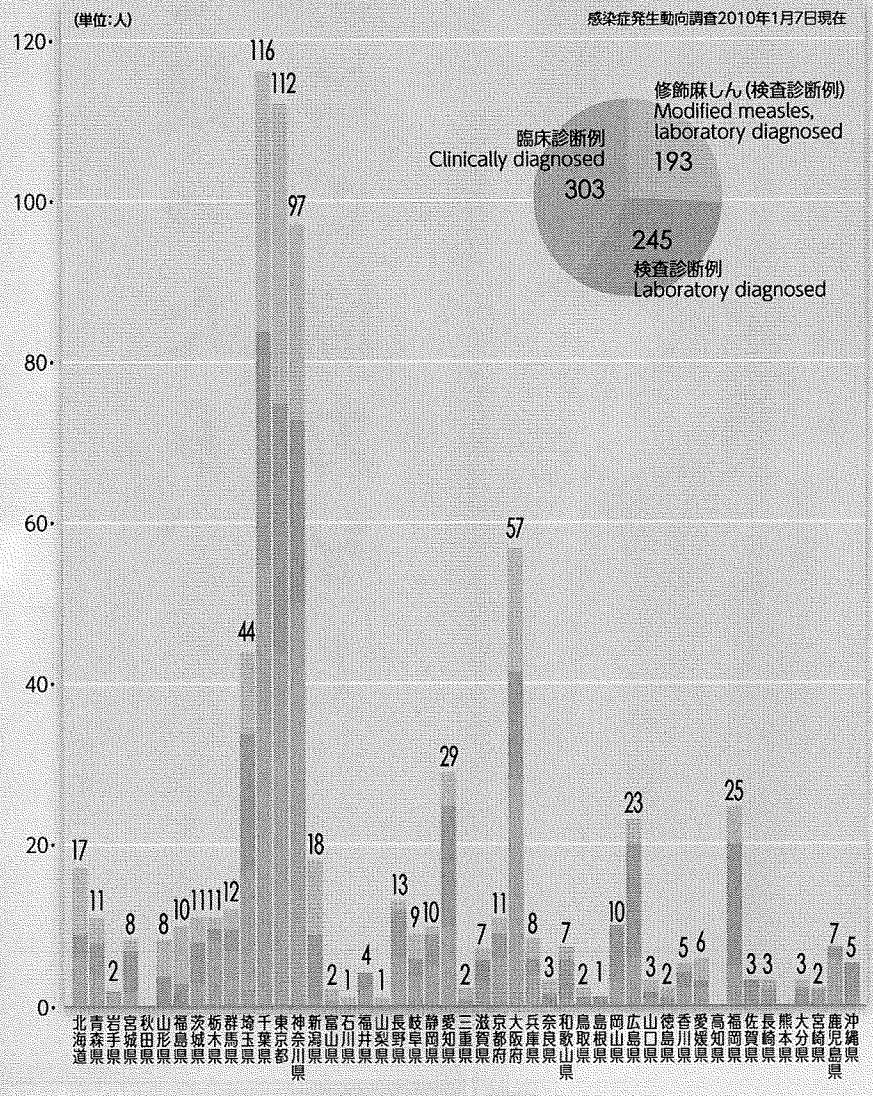

地方感染症研究所と国立
検査診断体制を整備して

予防接種が普及し患者数が大きく減少すると、相対的に予防接種歴ありの修飾麻しんの割合が増加します。修飾麻しんは臨床症状のみでの診断は困難であり、検査診断の重要性が増しています。
また、IgM抗体検査のみでは偽陰性、偽陽性があり、結果の解釈に注意が必要です。
そこで、日本は世界の麻疹風疹実験室ネッ
全国
究所
ンタ
る検
らて
じて
研究
体制

2 検体受け入れのフローチャート

麻しんの検査診断の4つの方法と注意点

❶ 急性期の麻しん特異的IgM抗体陽性（発疹6～10
（富樫：病原微生物検出情報. 31 (2) :11-12,2010 参照 http:/
❷ 急性期と回復期のペア血清で麻しん特異的IgG
❸ 咽頭ぬぐい液、尿、血液のいずれかから、麻しん
タイムPCR法など）
❹ 咽頭ぬぐい液、尿、血液のいずれかから、麻しんウ

しかし、注意しなければならないのは、以下の3点で
（中村：病原微生物検出情報. 31 (2) :12-13, 2010 参照 http://ic

❶ 発症初期（発疹出現後4日以内）では、麻しんであ
場合があります
※麻しんであれば日を改めて再度検査すると陽性にな
❷ ヒトヘルペスウイルス6（HHV-6）による突発性
ング熱等のウイルス感染症の急性期には、麻しん
陽性に出てしまう場合があります
※麻しんではないので再度検査しても値は上昇せず、
ルスの検出もなされません
❸ 修飾麻しんでは麻しん特異的IgM 抗体が陰性の
※RT-PCR法などで麻しんウイルス遺伝子が検出できる
から著明高値の場合があります

これらのことから、医療機関で麻しんを疑った場合
な検査診断を実施することが求められています。
れると、輸入例かどうかの判断がつく場合もありま